Status of the Compressed Baryonic Matter (CBM) experiment at FAIR

N. Herrmann[1], for the CBM collaboration

[1]Physikalisches Institut, Univ. Heidelberg, Heidelberg, Germany

The exploration of the QCD phase diagram in the region of high baryon densities is the primary goal of the physics program of the Compressed Baryonic Matter (CBM) experiment at FAIR.

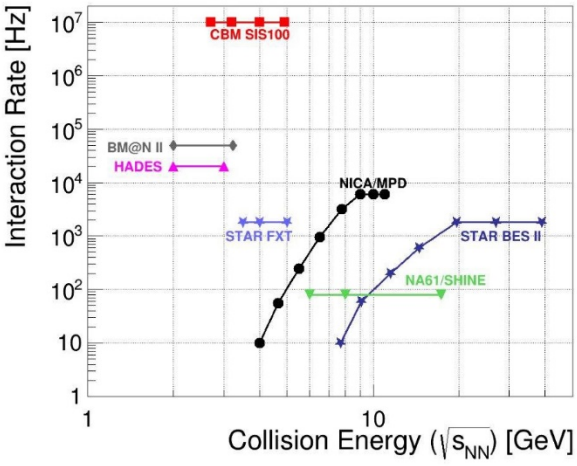

Figure 1: Rate capabilities as function of collision energy of existing experiments and experiments under construction.

In order to make substantial progress beyond existing data and currently running experiments the CBM experiment is designed to be operated at extremely high reaction rates of up to 10 MHz. This unprecedented rate capability allows to perform unique systematic measurements of multi-differential observables and at the same time the measurement of rare diagnostic probes. Figure 1 depicts a comparison of the interaction rates of existing and future heavy-ion experiments as function of collision energy.

The planned experimental setup shown in Fig. 2 is designed to address all observables that are currently employed in our research field to quantify QCD matter properties. Towards that goal CBM can be operated in various configurations, most notably two different base configurations are being prepared: i) the electron - hadron setup that allows the simultaneous measurement of electrons, positrons and charged hadrons, including all mother particles that have decay branches into these particles, and ii) the muon setup that focusses on the measurement of dimuon pairs originating from vector mesons including charmonium and the continuum exhibiting the same quantum numbers.

The key for high-rate operation are fast and radiation hard detectors, and a data acquisition and analysis concept that allows to enhance the rare probes to the level of significant results while keeping and characterising the accompanying features of the surrounding bulk matter. This will be achieved by a system without a traditional hardware based trigger system. All data items from the sensors will receive a time stamp and will be forwarded by the DAQ system in the so-called free streaming mode to a high performance computing cluster where event building and event selection occurs in real time.

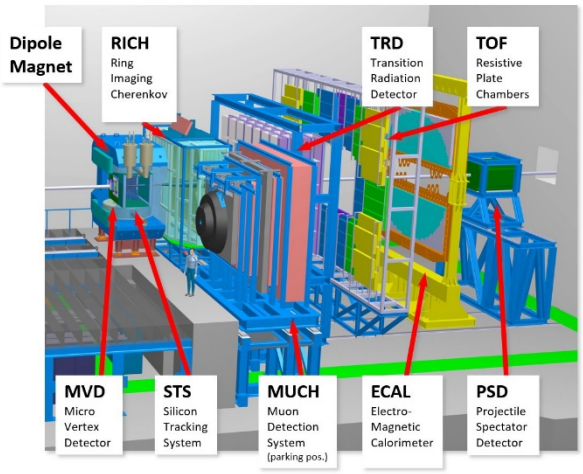

Figure 2: Overview of the CBM experimental setup. The experiment comprises high precision tracking by the MVD and STS detector systems in the magnetic field of a superconducting dipole magnet, event characterisation by a projectile spectator calorimeter (PSD) combined with two different detector arrangements for particle identification. Shown is the electron hadron setup in measuring and the muon setup in waiting position. For further details, see text.

The overall timeline for the construction and installation of the CBM experiment was adapted to the new FAIR baseline planning with the major milestones:

Dec 2021 - CBM building ready for infrastructural installations

Dec 2022 - CBM building ready for installation of components

Jun 2024 - First commissioning beam from SIS100 In the following recent developments of the overall CBM concept and its realisation are highlighted.

Detectors

On the detector side the Technical Design Report (TDR) for the last missing major component with large production time demands, the Transition Radiation Detector (TRD) was completed in 2017 and submitted to the FAIR ECE. A system of 4 layers of TRD chambers is

proposed that was shown to be efficient for achieving the physics goals:

i) electron - pion separation with a pion suppression factor of 20 at 90% electron efficiency in the momentum range beyond 5 GeV/c and ii) separation of nuclear charges e.g. for distinguishing deuterons from α - particles.

All other detector systems are as well on track to meet the FAIR timeline presented above.

Data Processing System

CBM is developing a high throughput data acquisition system that is based on the GBTx frontend ASIC developed at CERN. During the past year this system got further refined by shifting the long distance data transport task to commercial (Infiniband) components. Thus the former data processing board (DPB) and the FLES interface board are merged into a new component, the Common Readout Interface (CRI). The layout of the data processing system is shown in Fig.3.

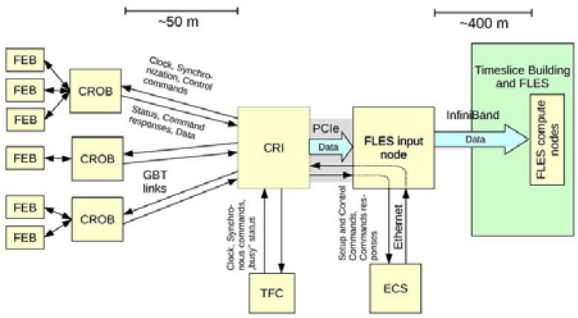

Figure 3: Schematics of the CBM data acquisition and pro- cessing system. Acronyms: FEB - Front End Board, CROB

- Common Readout Board, CRI - Common Readout Interface, TFC - Timing & Fast Control, ECS - Experiment Control System, FLES - First Level Event Selector

The CRIs will be placed into FLES input nodes that are part of the CBM experimental setup and are located in the counting house of CBM. The interface to the Online compute farm housed in the GreenCube of GSI/FAIR will be provided by a high performance Infiniband switch.

Computing

The execution of a high rate experiment like CBM that implements all data selection steps in software requires a software framework that is flexible, scalable and makes use of the latest hardware development. In order to accommodate the various tasks the computing effort within CBM was restructured and a Computing Board (COB) was installed.

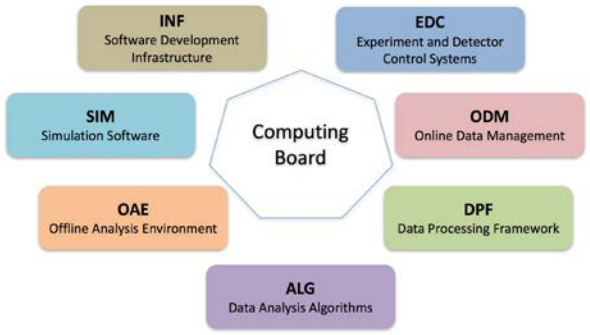

Further details can be found in the corresponding chapter of this report.

Physics Performance

The physics goals of CBM encompass all relevant observables for studying the QCD equation of state, the signals for a possible phase transition, investigation of a possible critical point, chiral symmetry restoration at large baryon chemical potential and the search for rare (quasi) bound states of QCD. These observables are described in detail in the recent CBM publication [1].

The evaluation of the physics capabilities of the CBM experiment is being continued and extended e.g. with detailed studies of the reconstruction of neutral pions, weak decays with neutral daughter particles and evaluation of the accuracy of directed flow measurements.

FAIR Phase-0 Program

Due to the delay of the overall FAIR completion FAIR council has endorsed the usage of CBM detector components and the participation in running experiments, especially at the GSI site making use of the beams available from the SIS18 synchrotron.

Currently CBM groups are pursuing the following projects within the framework of FAIR phase-0:

1) Participate in the HADES experiment at SIS18 by providing an enhanced performance of the HADES RICH detector by employing a readout with CBM owned MAPMT photo sensors.

2) Participate in the Beam Energy Scan II (BES-II) campaign of the STAR experiment at the RHIC at BNL, USA by installing 10% of the final CBM - TOF modules as endcap time-of-flight system, significantly extending the phase space coverage of the experiment. [2]. In addition, CBM high performance tracking software will be used for elaborating efficient data processing.

3) Participate in the BM@N experiment at the Nuclotron accelerator of JINR with the installation of 4 STS tracking

DOI:10.15120/GR-2018-1

stations in order to enhance the momentum resolution of the setup and with the PSD detector for better event characterization.

4) Install and operate a CBM test facility (mCBM) at the SIS18 accelerator of GSI in order to develop and verify the full data acquisition and analysis chain of the CBM experiment (see next section).

The FAIR phase-0 programs will be terminated at latest in 2023, afterwards shifting the core activities to the preparation of running at SIS100. The experience gained during the phase-0 program will certainly help to minimize the commissioning time needed to get full CBM online.

mCBM

mCBM is a test installation of CBM in order to evaluate the performance of detector and data acquisition and analysis components for their full functionality under realistic load conditions at the SIS18 accelerator of GSI [3]. The conceptual design of the experiment is shown in Fig.5.

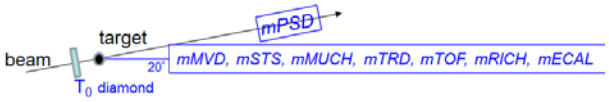

Figure 5: Conceptual layout of the mCBM experiment

mCBM is designed to explore the rate capability of all detector components arranged in a telescope like. Prototype and preproduction modules of MVD, STS, MUCH, TRD, TOF, RICH and ECAL will be placed under a scattering angle of about 20◦ with respect to the beam direction. In addition, one module of the PSD will be placed under the primary beam pipe at an angle of 5 degrees with respect to the beam direction. All detectors will be read out by a common triggerless data acquisition system. A dedicated link into the GreenIT cube to a mFLES cluster will be provided to exercise data transport and analysis.

The experiment is being prepared in the HTD area of the SIS18 experimental hall. No magnetic field will be available at the target spot.

One of the goals of mCBM is the validation of the CBM analysis concept that has to perform under real time conditions. The performance can and will be evaluated ma- king use of (sub)threshold Λ - baryon production in Ni + Ni (1.93A GeV) and Au + Au (1.24A GeV) collisions with cross sections available in literature. However, the unique and distinguishing feature of CBM, that has been worked out in the context of the proposal [3], is that spectra like the ones shown in Fig.7 have to be accumulated within 10s beam on target.

This report is also part of the CBM Progress Report 2017 (doi:10.15120/GSI-2018-00485)

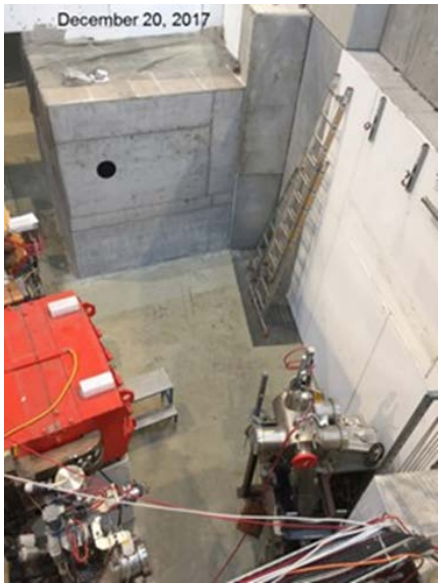

Figure 6: Cave of the mCBM experiment. A new beam dump surrounding the nominal beam position visible as a black circle had to be designed and constructed to enable the planned beam particle flux of 108 Au - ions per second at the highest SIS18 energy.

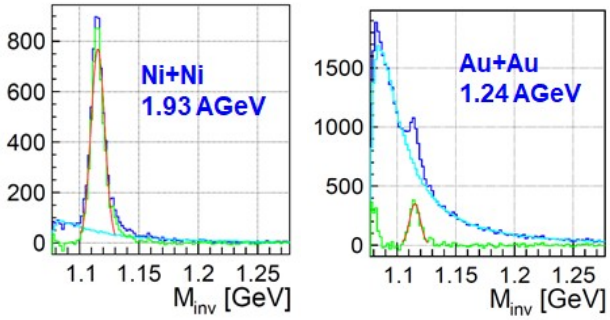

Figure 7: Benchmark observables for the mCBM experiment.

References

[1] T. Ablyazimov et al. (CBM Collaboration), “Challenges in QCD matter physics - The scientific programme of the Compressed Baryonic Matter experiment at FAIR”, Eur.Phys.J. A53 (2017) 60

[2] STAR and CBM - eTOF collaboration, “Physics Program for the STAR/CBM eTOF Upgrade”, arXiv:1609.05102v1 [nucl- ex]

[3] https://cbm-wiki.gsi.de/foswiki/bin/view/Public/Documents#mcbm 45proposal2GPAC 45fullVersion.pdf

Experiment beamline: SIS18-CaveC
Experiment collaboration: CBM
Experiment proposal: S471
Accelerator infrastructure: SIS18 / SIS100 / RHIC / Nuclotron
PSP codes: 1.1.1

Grants: see individual contributions
Strategic university co-operation with: Darmstadt / Frankfurt-M / Gießen / Heidelberg

 DOI:10.15120/GR-2018-1

The superconducting dipole magnet of the CBM experiment

P. Senger and the CBM collaboration

GSI, Darmstadt, Germany;

Magnet parameters

The magnet has a free aperture of 1.44 m vertically and 3.0 m horizontally in order to accommodate the STS detector system with a polar angle acceptance of 25 degrees and a horizontal acceptance of 30 degrees. The total length of the magnet is 1.5 m. The maximum magnetic field in the center of the magnet is 1.08 T, and the field integral within STS detector is BxL = 1.004 Tm. The fringe field downstream the magnet has values of the order of 50 to 100 Gauss at a distance of 1.6 m from the target at the position of the first RICH detector box. The field clamps are dismountable for the MUCH. The magnet can be operated as both polarities. The magnet is of the H-type with a warm iron yoke/pole and cylindrical superconducting coils. The wire has Nb-Ti filaments embedded into a copper matrix with a total Cu/SC ratio of about 7.1. The operating current and the maximal magnetic field in the coils are 686 A and 3.9 T, respectively. The coil case is made of stainless steel. The vertical force in the coils is about 250 tons. The cold mass is suspended from the room temperature vacuum vessel by six suspension links. Six cylindrical support struts compensate the vertical forces. The energy stored in the magnet is about 5 MJ.

Magnet design

The 3D magnetic field calculations were made with the Mermaid code, whereas the forces on the coils and the poles were calculated with the ANSYS 2D model. It was found that the calculated stresses in the coil structure and inside the windings are found to be well below acceptable stresses in stainless steel, copper, and the NbTi superconductor. The cross section of the iron yoke is shown in figure 1. The iron yoke serves as a construction frame for the magnet and systems of the detector. The total mass of the iron yoke is about 140 tons. It has special tools for adjusting its position in all directions. The yoke is assembled of iron blocks having masses in the range between 3 and 13.6 tons. The magnet comprises two separated superconducting coils symmetrically placed close at the top and bottom blocks of the iron yoke. The coils are placed around the cylindrical pole shoes of the magnet.

The lower coil is shown in figure 2. The main components of the coils are superconducting cables, the copper and the stainless steel cases. The copper case has a U-shape profile, and will serve as a bobbin during a winding procedure of the coil. The stainless steel case will be assembled around the copper case after finishing of the winding procedure. The parts of the stainless steel case will be bolted together. Each coil will be made of two pieces of superconducting cable each with a length of about 4.5 km. The splicing will be made during a winding procedure of one coil using soft soldering on a base of Sn-Ag alloy. The coils will cooled indirectly by a flow of liquid helium at 4.5 K through a tube which has an internal diameter 16 mm and wall thickness 2 mm. These tubes will be imbedded in the copper case such that the exit end of the tube is placed at a higher position than the inlet end of the tube (see figure 2). In this case the helium bubbles will accelerate the total helium flow along the tubes. If necessary, this thermosyphon cooling concept can be improved by additional heaters at the outlet of the tubes. The design includes the complete cryogenic system including the branch box, helium transfer line, the cryostat and the feed boxes, as well as the power supply and the quench detection and protection system. The magnet will be built by the Budker-Institute for Nuclear Physics (BINP) in Novosibirsk.

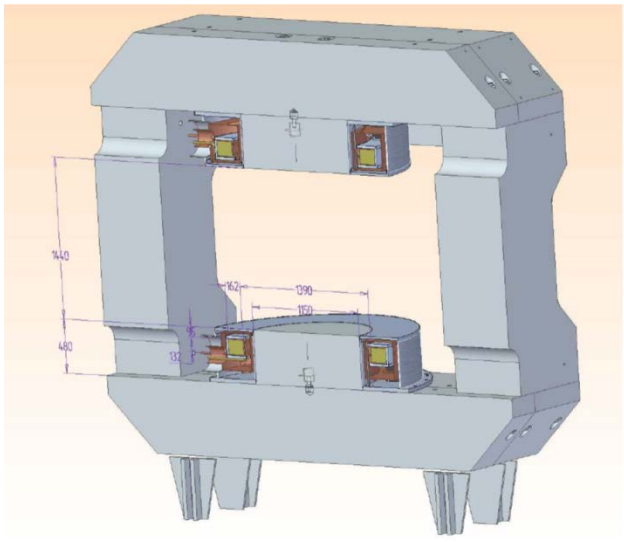

Figure 1: Cross section of the CBM superconducting dipole magnet.

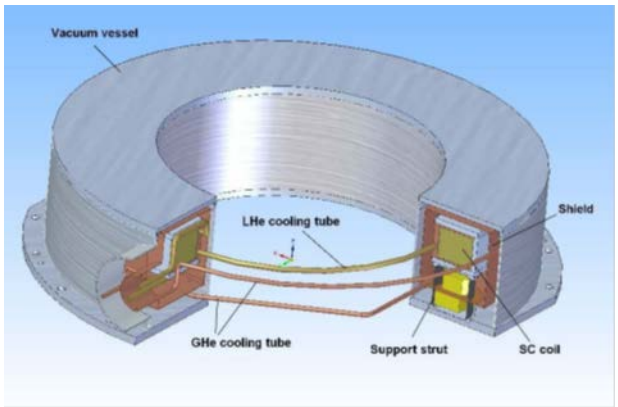

Figure 2: Total view of the lower coil of the CBM magnet (for explanation see text).

DOI:10.15120/GR-2018-1

CBM Micro Vertex Detector - Summary

C. Müntz, J. Stroth, and the CBM MVD working group

Goethe University Frankfurt, Germany; GSI, Darmstadt, Germany

The R&D carried out by the MVD team in 2017 focused on the design of the next generation pixel sensor MIMO- SIS and a review of the detector geometry. Moreover, the detector integration and slow control was studied in a dedicated research program. Radiation tolerance studies aimed to enable MAPS to resist the excessive radiation levels considered for a future MVD detector upgrade.

Sensor R&D and detector geometry review

Given the progress in sensor technology, is has recently decided to abandon the rolling shutter readout and to equip the MAPS sensors for CBM with the faster priority encoder readout, which was previously developed for the ALICE APIDE sensor. Among the benefits of the technology choice is an acceleration of the time resolution of the sensor by one order of magnitude, which turns into a proportional decrease of the detector occupancy and easier event reconstruction. Despite of this benefit, ALPIDE does not reach the radiation tolerance and data bandwidth needed for CBM. Therefore, a dedicated CBM sensor named MI- MOSIS is being developed. A first small size detector prototype MIMOSIS-0, which integrates updated pixel cells and priority encoders was designed at the IPHC Strasbourg and fabricated in 2017. Moreover, a dedicated test bench has been build. The necessary sensor tests will be carried out at the Goethe University Frankfurt and the IPHC Strasbourg in 2018.

The novel MIMOSIS sensor is projected to show different dimensions than the previously considered design. Therefore, an update of the MVD geometry and of the related simulation model was required. The updated model was build based on new scripting tools for CbmRoot. Two geometries, one optimized for vertexing and one optimized for low momentum tracking, were generated and their tracking performance was simulated. Preliminary results suggest that the tracking geometry provides indeed an improved tracking performance, namely in case the field of the CBM dipole magnet is reduced below its maximum intensity.

Sensor Integration and slow control

The integration of sensor into a full detector station was studied with the ”PRESTO” (PRototype of thE Second sTatiOn) prototype. The assembling of the prototype, which is formed from a TPG support holding two layers of MIMOSA-26 sensor, dedicated flex print cables and a TRBv3-based readout, has been completed.

The resulting sensor integration yield after sensor assembly is, though based on very limited statistics, not yet satisfactory. The wire bonding quality was excluded to cause the observed yield. Instead, ESD issues due to possibly low relative humidity during assembly in our laboratory are considered as origin of the observed sensor malfunction. At present, corrective measures are being implemented. Here- after, a second PRESTO module will be assembled in the hope to obtain a significantly improved integration yield.

The existing prototype is now being used as a test system for validating thermal management concept and the vacuum compatibility of the device. Doing long term in-vacuum tests requires to equip the prototype with robust slow control and protection system. A suited system based on EPICS was designed, implemented and commissioned.

Radiation Hardness

While the tolerance of present MAPS to non-ionizing radiation is sufficient to match the requirements of the CBM MVD, only few safety margin is remaining. Therefore, and in the prospective of a future MVD upgrade, options for a further improvement of this radiation tolerance was studied. The strategy consisted in fully depleting the active volume of the sensor, which was previously shown to improve the charge collection efficiency of the damaged device decisively. However, intense cooling was required to operate the irradiated sensors, which was initially not understood. Studies carried out in 2017 revealed that in- creasing the depleted zone of the photo diodes of the sensors comes with draw backs in terms of increased leakage currents, which were compensated by the cooling. An alternative solution to handle this issue suggests employing a faster shaping/readout mechanism, which is in any case required for a potential detector upgrade. Studying this effect more quantitatively is considered to provide valuable guidance for the next steps of sensor R&D.

This report is also part of the CBM Progress Report 2017 (doi:10.15120/GSI-2018-00485)

Experiment beamline: mCBM@SIS18
Experiment collaboration: CBM
Experiment proposal: S471
Accelerator infrastructure: SIS18 / SIS100
PSP codes: 1.1.1
Grants: BMBF 05P16VTFC1
Strategic university co-operation with: Frankfurt-M

Status of the Silicon Tracking System

H. R. Schmidt[1,2], J. M. Heuser[2], K. Agarwal[1], O. Bertini[2], A. Chaus[3], S. Das[1], M. Dogan[2,4], U. Frankenfeld[2], E. Friske[1], J. Hoffmann[2], M. Kis[2], K. Koch[2], P. Koczon[2], E. Lavrik[1], J. Lehnert[2], A. Lymanets[2], H. Malygina[2,6], O. Maragoto Rodriguez[2,6], S. Mehta[1,2], I. Momot[2,6], I. Panasenko[1,3], V. Pugatch[3], A. Rodriguez Rodriguez[2,6], Ch. Schmidt[2], C. Simons[2], M. Teklishyn[5], R. Visinka[2], O. Vasylyev[2], A. Weis[2], A. Wilms[2] for the CBM Collaboration

[1]Universität Tübingen, Germany, [2]GSI, Darmstadt, Germany, [3]KINR, Kiev, Ukraine, [4]Istanbul University, Turkey, [5]FAIR, Darmstadt, Germany, [6]Universität Frankfurt, IKF, Germany

The Silicon Tracking System (STS) of the CBM experiment will provide standalone charged-particle trajectory measurement and associated momentum determination, thus being the key detector in any phase of the CBM physics program, from the beginning of operation.

In this chapter of the Scientific Report, the STS work group teams from Germany, Poland, Russia and Ukraine give a cross section of the achievements made in the last year in the various fields of activities. On the chapter's title page, the depicted "mini STS" set-up for operation in the precurser project mCBM@SIS18 illustrates that the finalizing developments move from the component level to prototyping composite structures and their application in demonstration systems, prior to the start of series production of the CBM-STS parts after a number of readiness reviews in 2018.

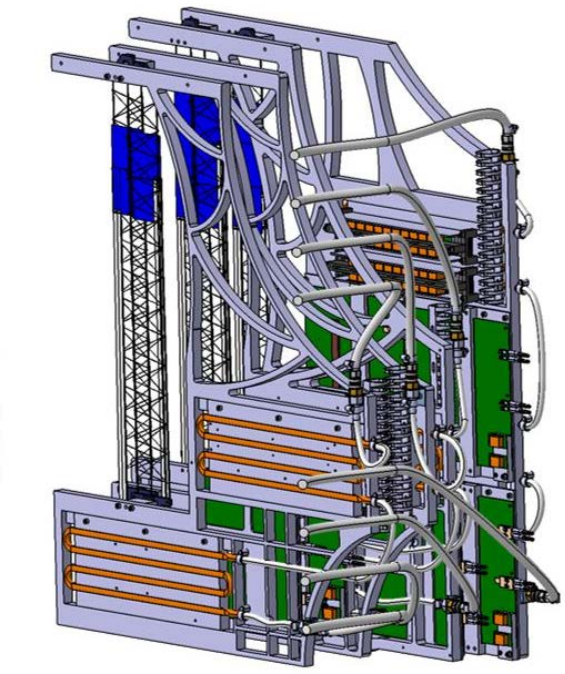

Figure 1: Sketch of the mSTS set-up planned for operation in the pre-curser project mCBM@SIS18.

The CBM Silicon Tracking System

The STS detector has been laid out to achieve the track reconstruction task (beam-target interaction rates up to 10 MHz, charged track multiplicities up to 700 per central Au+Au collision, momentum resolution of $dp/p \approx 1.8\%$, detection of strangeness by in-flight decays) with eight low-mass tracking layers in a 1 Tm dipole magnetic field covering the CBM aperture of $2.5^\circ < \theta < 25^\circ$, corresponding to rapidities ranging from mid rapidity to close to beam rapidity. The sensor technology is based on double-sided silicon wafers with microstrip segmentation. The readout strip pitch of 58 μm under 7.5° stereo angle realizes single-hit resolution of about 25 μm. The read-out is based on self-triggering front-end electronics streaming time-stamped data to a computing farm for on-line hit sorting, track identification, event forming and analysis. To minimize material budget in the acceptance region, the STS has been designed such that front-end read-out electronics, cooling and mechanical infrastructure are located outside of the physics acceptance. The detector modules employ ultra-thin microcables for separating those from the sensors. Four sensor variants (6.2 cm wide, 1024 strips per side, and 2.2/4.2/6.2/12.4 cm long, with the corresponding strip lengths matched to the hit densities at their respective positions) and different microcables up to 50 cm lengths result in 18 module variants to be constructed, 896 modules total. Eight or ten modules are integrated onto a detector ladder. The STS will comprise 106 detector ladders that are mounted on 18 mechanical units within the STS space frame, forming the tracking stations. The modules and ladders for the 4 upstream tracking stations are to be assembled at JINR VB-LEHP, those for the 4 downstream stations at GSI, where also the system assembly will be done. The detector's front-end and powering electronics will dissipate about 40 kW of power. Efficient heat removal through cooling plates circulating bi-phase CO_2 will be applied. The sensors will be operated at up to 500 V bias, at a temperature of around -5 °C to limit radiation damage induced leakage currents from the integrated lifetime fluence of up to 1×10^{14} cm^{-2} 1-MeV neutron equivalent in the regions close to the beam axis. The STS will thus be housed in a thermally insulating enclosure, incorporating feed-throughs for low and high voltage supply, optical and control links. A section of the vacuum beam pipe will cross the detector, made from 0.5 mm thick carbon fiber/foil layers, attaching to the target vacuum box on the beam upstream side and to

the downstream STS wall with further connection towards the RICH or MUCH detectors.

Progress with silicon microstrip sensor

The final prototypes of the STS silicon microstrip sensors have been developed. The four main variants with strip lengths matched to particle densities in the STS and the layout optimized for module assembly have been produced in small series with two vendors (CiS, Erfurt, Germany; Hamamatsu, Japan). The technical specifications and quality criteria are fixed. Radiation tolerance has been demonstrated in various tests on specimen irradiated up to twice the lifetime fluence. An internal sensor review was held in March, 2017, covering all aspects of required specifications, their realization, performance, quality assurance, capabilities of vendors. One open work item was identified: the demonstration of sensor performance (charge collection, signal-to-noise ratio, efficiency for track finding) in a realistic prototype module structure with the sensor tab-bonded to microcables and STS-XYTERv2.0 ASIC. This test took place in the in-beam test at COSY in February 2018. The production readiness review is planned for April 2018 and the call for tender in the second quarter of 2018

Progress with module assembly

The assembly of sensors, microcables and front-end electronics boards into the basic building block of the STS, the detector module, has been developed. The workflow for the double-sided handling has been established, assembly tools have been designed and manufactured, last improvements are being made for the modules to be assembled for the mSTS in 2018. The production site at GSI is equipped and ready for production. Likewise, at JINR where the module assembly with two daisy-chained sensors replacing the largest prototype has been studied. The specifications for the microcables with aluminum traces are almost fixed. Microcables with Copper traces have been ordered in industry and will be tested as an alternative. An internal production review is planned for July 2018.

Progress with ladder assembly

Ladders are the mechanical assemblies of detector modules onto carbon fiber support structures that will be attached to the mechanical units. Carbon fiber prototype structures with varying specifications have been produced with two companies in Germany and Switzerland; a third producer is to be tried. A work flow for ladder assembly has been established at GSI and the required module placement precision ± 35 μm demonstrated, using an optical survey machine installed there. The next iteration of the tools will address the ladders to be produced for mSTS. An internal review on ladder assembly will be held jointly with the module assembly review in July 2018.

Progress with front-end and read-out electronics

In preparation of the final STS front-end chip, STS-XYTERv2.1, detailed studies of the prototype v2.0 have been carried out. For the first time, hundreds of ASICs have been screened and the high production yield determined. Detailed insight into the performance of the analog and digital building blocks has been gained through dedicated measurements. Particular focus has been put on understanding the different loads and their influence on noise. Several substantial modifications to the analog front-end and to the digital back-end will be implemented for the submission in 2018. A first prototype of the front-end board holding 8 ASICs has been designed and produced at GSI. In a module, a left and a right-handed version are required. The prototypes are required for the mSTS modules in 2018. For the read-out of the FEB-8, the GBT protocol has to be used. A first prototype of the read-out board ("Common ReadOut Board", CROB) with GBTX ASICs and VersatileLink optical modules is under test. A prototype link cable for the transmission of data from the front-end to the read-out board has been produced and tested.

Progress with system integration and mSTS demonstrator

The system integration team has addressed various aspects of this wide topic. The STS CAD model is already quite detailed. Its finalization is ongoing, starting with a final confirmation of the sensor positions in a physics performance simulation study and subsequent freezing of all details of the module and ladder variants as well as the detailed dimensions of the mechanical units. A mechanical demonstrator of a quarter C-frame has been finished, allowing decisions regarding ladder mounting technology, mechanical precision, ladder installation, cabling in the detector. The routing of cables from the detector to the supplies in the CBM cave has been addressed. A cooling demonstrator under study addresses the feed-through panels in the thermal wall for HV/LV/data/control links, thermal interfaces for efficient cooling of the electronics, and cooling of the sensors. A first prototype of the STS beam pipe section has been produced and awaits vacuum stability tests. Simulation studies address detector alignment based on tracks to achieve higher-than-intrinsic mechanical precision of sensor positioning for physics measurements. Several aspects of system integration, as well as detector module operation and read-out ASIC performance, are to be demonstrated before production readiness with the "mini STS" (mSTS) in the "mini CBM" (mCBM) set-up. The primary purpose of mCBM is to prove data transport/event building in technical runs in 2018/2019, with potentially further physics runs in 2020/2021. As this requires realistic input from prototype CBM detector systems ("sectors"), the mSTS has been conceived, implementing two small tracking stations with two and three ladders (four and nine modules), on a somewhat simplified mechanical structure. Electronics cooling will be implemented and tested but the sensors will be operated non-cooled at ambient temperature as the radiation load will be non-critical. The mSTS specifications have been frozen and the design is close

 DOI:10.15120/GR-2018-1

to full detailing. Production of the components will start in March 2018

STS project plan

A detailed STS project plan has been established from the current pre-production phase, over test-experiments, production readiness reviews in 2018, the construction phase from 2019 to 2022 and readiness for STS installation into the CBM cave in 2023. It comprises milestones and is an official planning document within the FAIR project. The planning has been matched with a detailed cost assessment and spending profile, backed up by contracts between the participating project partners.

This report is also part of the CBM Progress Report 2017 (doi:10.15120/GSI-2018-00485)

Experiment beamline: mCBM@SIS18
Experiment collaboration: CBM
Experiment proposal: S471
Accelerator infrastructure: SIS18 / SIS100
PSP codes: 1.1.1
Grants: BMBF 05P16VTFC1
Strategic university co-operation with: Frankfurt-M

stsDPB firmware development - preparations for CRI

W.Zabołotny[1], A.Byszuk[1], M.Gumiński[1], G.Kasprowicz[1], K.Poźniak[1], R.Romaniuk[1]

[1]Institute of Electronic Systems, Warsaw University of Technology, Warszawa, Poland

New functionalities in the tester firmware

The firmware for the tester of MUCH-STS-XYTER 2 (SMX2) ASIC was further developed.

The implementation of the GBTX-based access to the SMX2 chip required serious rework of the SMX2 controller core. The GBT-IC/EC controller was delivered by the CERN GBT team and was integrated with the tester firmware. That allowed control of the phase of downlink clocks and delay of the uplink data via the optical link. Successful synchronization of e-Links and transmission of data was achieved. However, the I2C access to the GBTX chip is still needed for its initial configuration[1].

The support of ``time deterministic'' commands, needed for proper synchronization of the front-end ASICS has been added to the tester firmware and successfully tested.

Development of the stsDPB firmware

Even though the final solution for the CBM readout will be the Common Readout Interface (CRI) board, the Data Processing Boards (DPBs) are needed for development and test purposes. Therefore, the functionalities tested in the tester firmware were integrated into the stsDPB firmware initially developed by Junfeng Yang. Additionally, some new functionalities have been implemented directly in that firmware.

The tester firmware supports only a single SMX2. In the stsDPB, it was required to add support for multiple SMX2 chips.

That resulted in the reorganization of the firmware, modification of the block used to generate the phase-shifted downlink clocks, and modification of the Python procedures so that adjustment of one downlink does not corrupt state of the SMX2 ASICs connected to other downlinks. In particular, the downlink transmitter had to be completely stopped when the clock phase was adjusted. The Python procedures have also been refactored and supplemented with extensive logging functionalities.

Another task was the integration of the FLIM module with the stsDPB firmware. New functions for sorting and splitting the received data into microslices were added. A dedicated sorting system [1], shown in figure 1, was developed to merge multiple streams of sorted 32-bit data into a sorted output stream of 32-bit data at 320 MHz, without a necessity to operate complex sorters at so high clock frequency. The final sorter-merger performs the

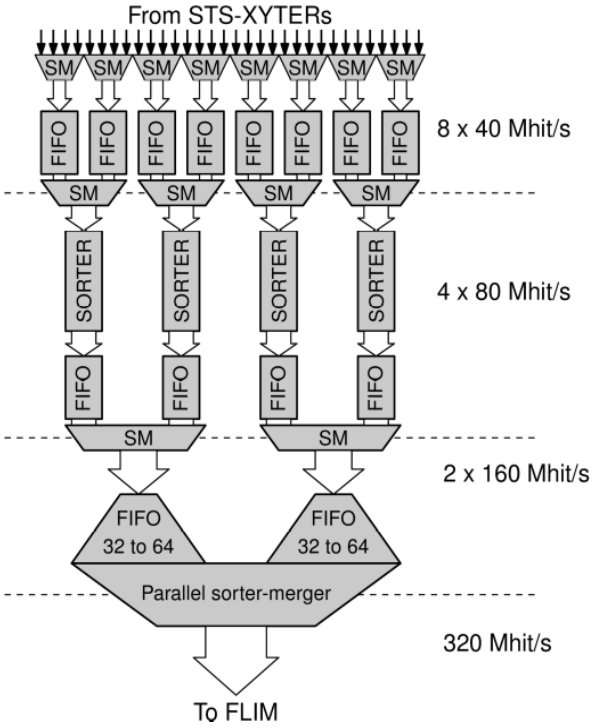

Figure 1: Structure of the data concentration system developed for stsDPB (SM - simple mergers).

comparison of 4 data words in parallel, selecting two oldest in a single 160 MHz clock cycle, producing the sorted stream of 32-bits words at 320 MHz.

The sorted data stream is split into Micro Slices and send via FLIM module to FLES.

Preparation for CRI

As a preparatory step for the development of the CRI boards, a review of available hardware solutions for the PCIe-based readout system was performed [2]. The results of this review allowed defining the viable configurations of the CRI boards and contributed to selection of the HTG-Z920 board as the first prototype of the CRI board.

1 The initial configuration of the GBTX provides settings needed to establish the connection via the optical GBT link. In the final setup the initial configuration will be read from e-Fuses. Because programming of e-Fuses is an irreversible operation, they could not be used at the development stage.

 DOI:10.15120/GR-2018-1

References

[1] M. Gumiński, “High-speed concentration of sorted data streams for HEP experiments”, presentation at Nica Days 2017

[2] W.M. Zabolotny et al., “Selection of hardware platform for CBM Common Readout Interface”, Proc. SPIE 10445 (2017) 1044549, doi:10.1117/12.2280938

Experiment beamline: none
Experiment collaboration: CBM
Experiment proposal: none
Accelerator infrastructure: none
PSP codes: none
Grants: Agreement between GSI and WUT “Development and implementation of a readout and control protocol between STS-XYTER and further data processing FPGA-based electronics for FAIR”
Strategic university co-operation with: none

Data transmission line for STS detector readout system

P.Koczon, J.Hoffmann[1], M.Kis, K.Koch[1], C.J.Schmidt, A.Weis

for the CBM collaboration FAIR@GSI and RBDL

[1] EEL GSI, Darmstadt, Germany

The silicon tracking detector STS for the CBM experiment @ FAIR/GSI in Darmstadt will consist of 900 double sided strip sensors and will register up to 10^7 events/sec of average multiplicity of 350. It will produce about 1 TB/s of data which has to be collected from 14000 front end ASICs (CBMxyter [1]) by a readout system based on the GBTx chip set [2]. The chips' specifications impose certain requirements on the quality of the data link between CBMxyter and GBTx which is proven for the concrete hardware realization in this work.

Test system for the link cable

The cable projected for the data transfer (Sumimoto Electric Interconnect) consists of 20 pairs of LVDS links and is 800 mm long and 20.5 mm wide. It has a strip pitch of 0.5 mm. These parameters were chosen to fulfil the STS@CBM specifications. Links are placed on one surface of a polyester supporting tape and shielded with aluminium foil along the entire length. The shielding can be grounded via extra pads at the cable ends. The cable ends are equipped with stiffening SUMI-CARDS fitting into 0.5 mm pitch horizontal ZIF FH41-40S-0.5SH(05) receptacle of Hirose. For the necessary data rate performance tests an adapter PCB with SMA connectors was constructed which allows to use high frequency LVDS signals produced by CLOSY2 [3]. Signals are fed via SMA- and ZIF [4]-connectors into the flat band cable of 20 LVDS link pairs. To avoid reflections 100 Ohm terminators were used on the end of the cable.

Test results

The signal propagation properties and the link quality of the link cable was proven through noise eye diagram measurement (Fig.1) and the cross talk measurements on side links (Fig.2). The horizontal opening of 1.25 ns of the very clean eye diagram obviously proves high quality of the cable under test to at least 800Mbit/s.

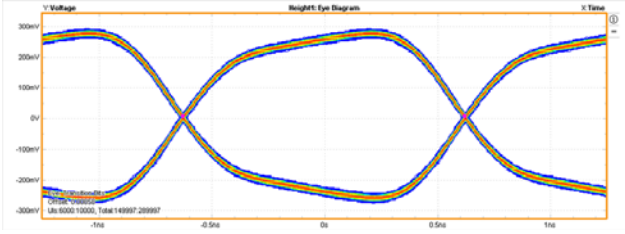

Figure 1. An eye diagram measured with DPO71254C Tektronix Oscilloscope at 400 MHz.

Fig. 2 shows very low cross talk between neighbouring links. Single ended signals are recorded on the end of the closest and second closest neighbour of an active LVDS link. The cross talk does not exceed 1% of the test signal height.

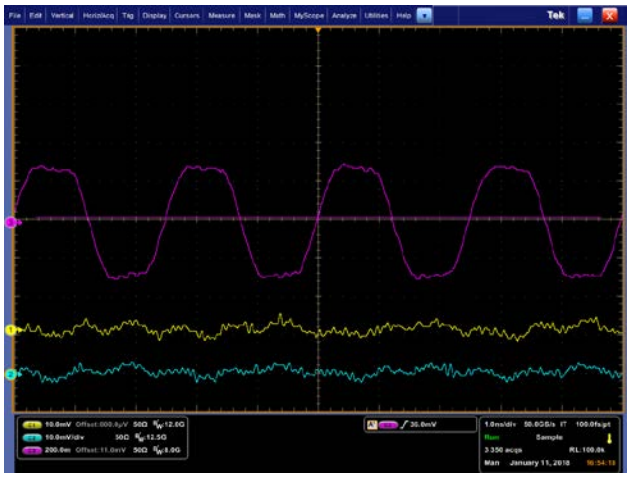

Figure 1. Crosstalk between one link carrying a *400 MHz LVDS signal and the neighbour*ing traces.

Conclusions

The symmetry of the eye diagram as well as the small RMS jitter of transitions together with very little crosstalk is a proof of high electrical quality of the tested LVDS cable. It seems that the cable can be used at still higher clock frequencies e.g. up to 800MHz and corresponding DDR rates of 1,6 Gbit/s, whereas 160 MHz (clk) and 320 Mbit/s is necessary for CBM.

References

[1] stacks.iop.org/1748-0221/11/i=11/a=C11018
[2] indico.gsi.de/event/3446/session/3/contribution/13/material/slides/0.pdf
[3] Helmholtz-berlin.de/media/media/spezial/events/sei/Desy10/koch_desy10_01.pdf
[4] hirose.com/product/en/products/FH41/FH41-40S-0.5SH%2805%29/

 DOI:10.15120/GR-2018-1

Summary Report of CBM RICH developments

J. Adamczewski-Musch[a], K.-H. Becker[b], S. Belogurov[c,f], J. Bendarouach[d], N. Boldyreva[e], C. Deveaux[d], V. Dobyrn[e], M. Dürr[d], J. Eschke[a], J. Förtsch[b], J. Heep[d], C. Höhne[d], K.-H. Kampert[b], L. Kochenda[e,f], P. Kravtsov[e,f], I. Kres[b], S. Lebedev[d], E. Lebedeva[d], E. Leonova[e], S. Linev[a], T. Mahmoud[d], J. Michel[g], N. Miftakhov[e], W. Niebur[a], J. Otto[d], E. Ovcharenko[c], V. Patel[b], C. Pauly[b], D. Pfeifer[b], G. Pitsch[d], S. Querchfeld[b], J. Rautenberg[b], S. Reinecke[b], Y. Riabov[e], E. Roshchin[e], V. Samsonov[e,f,h,] V. Schetinin[c], O. Tarasenkova[e], M. Traxler[a], C. Ugur[a], E. Vznuzdaev[e], M. Vznuzdaev[e], and A.A. Weber[d]

[a]GSI Helmholtzzentrum für Schwerionenforschung GmbH, Darmstadt, Germany;
[b]Department of Physics, University Wuppertal, Wuppertal, Germany;
[c]LIT JINR, Dubna, Russia;
[d]Institute of Physics II and Institute of Applied Physics, Justus Liebig University Giessen, Giessen, Germany;
[e]National Research Centre "Kurchatov Institute" B.P.Konstantinov PNPI, Gatchina, Russia;
[f]National Research Nuclear University MEPhI (Moscow Engineering Physics Institute), Moscow, Russia;
[g]Institut für Kernphysik, Goethe University Frankfurt, Frankfurt am Main, Germany;
[h]St. Petersburg State Polytechnic University (SPbSPU)

The CBM RICH project has made substantial progress in various fields in 2017 as will be presented in this report. First prototypes testing critical mechanical design issues of the RICH detector have been built. The RICH mirror wall is a sensitive part for the RICH detector as it has to combine high stability with low material budget. After discussing several conceptual ideas in 2015, an optimized design has been worked out in 2016 in which one pillar can support two rows of mirrors. In order to evaluate this design, a prototype pillar has been constructed in 2017 with 2 mm thick aluminum profile and successfully been tested for six months up to now with 150% of the expected load. The material budget of the small frames holding two mirrors each has been reduced by further 15-20% material budget. In parallel to ensuring highest stability from the mechanical part, software routines are in preparation in order to correct for any misalignment offline, should it happen to occur. In 2017 the full correction cycle was finally established showing that with software corrections remnant misalignments are on the level of 1 mrad which just fits to the specifications. Another critical design issue is the photodetector camera. A prototype ensuring a convenient construction of the cylindrical photodetector plane has been built and will be tested for stability, light and gas tightness in 2018. Unfortunately the shielding box of the photocamera remains to be an open design issue: The existing design could be adopted to the cylindrical photodetector plane, however partially blocks the acceptance of Cherenkov photons. In addition the redesign of the CBM magnet was not finished in 2017, the whole box has therefore to undergo a further iteration in 2018. The design of the RICH gas system was finalized and awaits the final approval. End of 2017 the last batch of the MAPMTs has been delivered by Hamamatsu. Within the first quarter of 2018 all 1100 MAPMTs will have been characterized. The RICH software underwent numerous changes to improve the realistic description, in particular quantum efficiency and sensitive area are now fully adopted to the chosen H12700 MAPMT. An important step forward was the implementation of an intermediate version of time-base RICH simulations. Within the next months this will be improved and tested 2019 with the participation of a mRICH detector in mCBM. A design of a mRICH prototype was developed and simulated reusing the testbox of the recent testbeam measurements at COSY. As radiator an aerogel tile will be used in order to enhance the pion-proton separation of mCBM.

The HADES RICH upgrade is running very well and driving the development of the RICH readout electronics. The first prototype of the RICH readout chain was available mid 2016, in 2017 an improved version was produced. This was tested in detail in the lab and could finally be fully verified in a testbeam experiment with proton beam at COSY. After initial problems with stability, the whole system was stable in the end and providing data with very low noise level. Automatic routines for threshold settings are available. First analysis of the data reveals that efficiencies are as expected from simulations, the time-over-threshold cut for noise suppression works successfully, and timing precision is on the order of 260 ps. Some MAPMTs were covered with WLS coating (p-terphenyl) in particular in order to measure timing properties. Results show a decay constant of 2.4 ns in agreement with time resolved fluorescence measurements. The previously increase of hit multiplicity of about 20 % was confirmed. Given these successful tests, the readout electronics was approved for mass production for the installation in HADES. The inner part of the photondetector will be coated with WLS films. Full installation is expected until the end of May 2018. The HADES RICH detector will then participate in the Ag+Ag beamtime of HADES in summer 2018 (FAIR phase 0) substantially enhancing the electron identification in HADES.

This report is also part of the CBM Progress Report 2017 (doi:10.15120/GSI-2018-00485).

Experiment beamline: mCBM@SIS18
Experiment collaboration: CBM
Experiment proposal: S471

Accelerator infrastructure: SIS18 / SIS100
PSP codes: 1.1.1
Grants: BMBF 05P15PXFCA, 05P15RGFCA, GSI
Strategic university co-operation with: Gießen

Summary on the CBM-TRD project

C. Blume[4,5], E. Bechtel[5], J. Beckhoff[8], A. Bercuci[1], N. Bialas[5], J. Book[5], V. Cătănescu[1], F. Fidorra[8], C. de J. García Chávez[8], S. Gläßel[5], M. Petrovivi[1], C. Şchiaua[1], S. Schreiber[5], H. Schuldes[5], D. Spicker[5], P. Kähler[8], L. Karalius[1,2], U. Kebschull[6], C. Klein-Bösing[8], M. Kohn[8], M. Krieger[7], A. Meyer-Ahrens[8], P. Munkes[8], I. Ouatu[1,3], F. Roether[5], R. Weihrich[5], the CBM collaboration, and the FAIR@GSI division

[1]National Institute for Physics and Nuclear Engineering (IFIN-HH), Bucharest, Romania; [2]Birmingham University, UK; [3]Oxford University, UK; [4]GSI, Darmstadt, Germany; [5]Institut für Kernphysik, Frankfurt am Main, Germany; [6]Infrastructure and Computer Systems for Data Processing (IRI), Frankfurt am Main, Germany; [7]ZITI, University of Heidelberg, Germany; [8]Institut für Kernphysik, Münster, Germany.

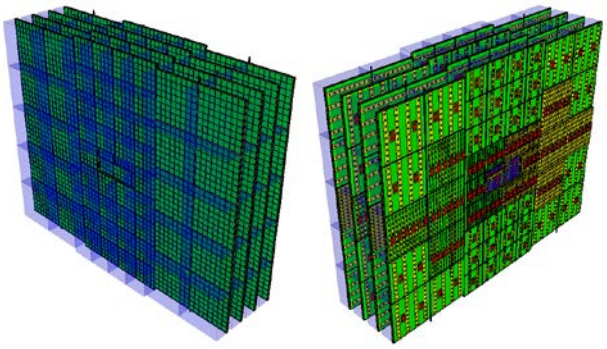

Figure 1: CBM-TRD geometry for SIS100, consisting of one station with four layers of detectors. Shown here is the implementation of the TRD geometry in the simulation framework. Visible are the ROCs with the radiator boxes in the front view (left), while the rear view (right) shows the backpanels of the ROCs together with the front-end electronics.

Introduction

The main task of the Transition Radiation Detector (TRD) is to identify electrons above momenta of 1 GeV/*c* and thus to extend the electron identification capabilities of the Ring Imaging CHerenkov (RICH) detector above momenta of $p \sim 5$ GeV/*c*. In this region the TRD should provide a pion suppression factor in the range of 10 – 20 at an electron efficiency of 90 %, in order to allow for a high quality measurement of dielectrons in the mass range from below the ρ and ω masses to beyond the J/ψ mass. Due to its capability to identify charged particles via their specific energy loss, the TRD in addition will provide valuable information for the measurement of fragments.

These requirements can be fulfilled with a Xe/CO_2 based Multi-Wire Proportional Counter (MWPC) detector in combination with an adequate radiator. The default MWPC design is composed of a symmetric amplification area of 3.5 + 3.5 mm thickness, complemented by a 5 mm drift region to enhance the TR-photon absorption probability in the active gas volume. This geometry provides also efficient and fast signal creation, as well as readout, with timescales below 200 µs per charged particle track. The performance of the detector is maximized by reducing the material budget between radiator and gas volume to a minimum.

The baseline design for the TRD at SIS100 will consist of one station, composed of four detector layers (see Fig. 1). It will be positioned between the RICH and the Time-Of-Flight (TOF) detector and thus will help to reduce the background in the TOF resulting from track mismatches by providing additional position information between RICH and TOF. The TRD will also be used as tracking station behind the last absorber of the MUCH detector in the muon configuration of CBM.

Technical design report

A first version of the Technical Design Report (TDR) for the TRD has been completed early in 2017. It was then scrutinized in an internal review in March 2017, which was performed by a committee of international experts on the various aspects of TRDs, electronics and the related physics topics. Based on the recommendations of the expert committee an extensive revision of the TDR and project was performed.

One major aspect of this process was the redesign of the TRD geometry with the aim of achieving an overall simplification. The new design, as shown in Fig. 1, now consists of only four (before six) different module types, two small ones (type 1 and 3, size 57cm × 57cm) and two large ones (type 5 and 7, size 99cm × 99cm). This facilitates the module production significantly and also allows for a simpler routing of service lines. Furthermore, many complications in the design of the readout system can now be avoided. E.g. only one type of Common ReadOut Board, namely C-ROB3, will now be required.

It was also decided to remove the chapter on alternative options from the TDR, such that the new version consistently describes a baseline solution for the whole TRD system. The innermost modules of the TRD, situated in the region of the highest hit rates, can still employ a different technology (i.e. pad planes with triangular pads and FASP readout), as being developed by the Bucharest group. This design will be described in an addendum to the existing TDR, which is currently under preparation.

The revised TDR has officially been submitted in Dec. 2017 to the ECE for the final approval.

Physics performance

The main physics cases for the TRD are the measurement of dielectrons in the intermediate mass range (i.e. between ϕ- and J/ψ-mass) and the identification of light nuclei. As a consequence of the TDR revision the corresponding physics performance studies had to be repeated with the

 DOI:10.15120/GR-2018-1

new TRD geometry and to be extended in order to address the referee comments. The results of the revised simulation studies are summarized in [7] (intermediate mass dielectrons) and [2] (identification of light nuclei). Both analyses were now done with three, four and five TRD layers in order to determine the optimal geometry for these physics observables. The results show that three layers would be insufficient, while an additional fifth layer is not needed to achieve the desired performance.

Front-end electronics

A test batch of the SPADIC 2.1 ASIC has been submitted. This version includes features suggested by the TDR referees, such as, e.g., an overload recovery and a running averaging for the baseline determination. It will have a BGA packaging in order to reduce the real estate occupied by the chip on the Front-End Boards (FEBs). This will allow to design FEBs which are small enough to fit flatly onto the backpanel of the TRD chambers, even for module type-1 which has the highest channel density.
The development of multi-ASIC FEBs is progressing well [3]. A first version of a quad-FEB, to be equipped with the SPADIC 2.0, is available and is intended to be used for mCBM.

Readout and feature extraction

The TRD readout has been upgraded for the connection of multiple SPADICS to a given AFCK board [4]. This implementation has been successfully tested at DESY and CERN-GIF and will be further extended for the quad-FEBs to be used for mCBM and for the GBTx-based C-ROBs.
An important part of the readout chain is the feature extraction stage, which will deliver event-filtered and bandwidth reduced data to the FLES. First performance studies on the online cluster reconstruction in terms of total cluster charge and position have been performed [5].

Laboratory and beam tests

Also in 2017 extensive test have been performed, both in the laboratory and at accelerators. The Bucharest group has set up a test stand equipped with a high intensity x-ray source, which allows to investigate the performance of prototypes under high counting rate conditions [6].
In Münster an automated calibration setup for the readout chambers using a Fe-source was build [7], which can be used for a quality assessment of newly produced readout chambers. This setup is currently also been used to study the multi-hit performance of the SPADIC [8].
A systematic test of four large prototypes with radiators was performed with electron beams at DESY [9]. These data allow for a detailed characterization of the radiators and will serve as a reference for the fine-tuning of the detector simulation.
In order to investigate the stability of the readout chambers and front-end electronics in a high rate environment a first test at the Gamma Irradiation Facility (GIF) at CERN was done [10].
The analysis of the test beam data of 2017 is currently still on-going. Several software developments on the software framework for the analysis of test beam data have been done [11], which now provide a unified environment for these studies.

Summary and outlook

With the finalization of the TDR the research and development phase for the TRD can almost be concluded. Ongoing activities mainly concern topics such as services, cooling and the gas system, while the design of the readout chambers themselves is essentially final. Four large chamber prototypes, which are already very close to this design and have already been operated at the CERN-SPS and DESY, will be available for mCBM. Also the development of the front-end electronics is progressing and final FEBs should be available by the end of 2018. Therefore, it is planned to start the production readiness review by the end of 2018 and to start mass production soon after that.

This report is also part of the CBM Progress Report 2017 (doi:10.15120/GSI-2018-00485).

References

[1] E. Bechtel et al., “Performance study on dielectron measurements in Au+Au collisions with the CBM-TRD”, CBM Progress Report 2017, p. 155.
[2] S. Gläßel et al., “Hadron identification via energy loss measurements with the TRD”, CBM Progress Report 2017, p. 156.
[3] F. Roether et al., “Front end board development for the CBM-TRD”, CBM Progress Report 2017, p. 86.
[4] C. de J. Garcia Chávez et al., “Status update of the TRD data acquisition chain during 2017”, CBM Progress Report 2017, p. 87.
[5] C. de J. Garcia Chávez et al., “Performance study of the feature extraction”, CBM Progress Report 2017, p. 88.
[6] A. Bercuci et al., “Laboratory tests of the TRD Bucharest prototype in close to realistic high counting rates (HCR) environment”, CBM Progress Report 2017, p. 89.
[7] J. Beckhoff et al., “Automated gain-table measurements for the CBM-TRD”, CBM Progress Report 2017, p. 91.
[8] M. Kohn et al., “Analysis of the SPADIC Multi-Hit feature”, CBM Progress Report 2017, p. 92.
[9] F. Roether et al., “Electron test beam campaign of the CBM-TRD at DESY”, CBM Progress Report 2017, p. 93.
[10] P. Kähler et al., “High-rate test of a CBM-TRD module at the CERN-GIF”, CBM Progress Report 2017, p. 94.

[11] P. Munkes et al., “A new in-beam-test data analysis framework for the CBM-TRD”, CBM Progress Report 2017, p. 95.

Experiment beamline: mCBM@SIS18
Experiment collaboration: CBM
Experiment proposal: S471
Accelerator infrastructure: SIS18 / SIS100
PSP codes: 1.1.1
Grants: BMBF-grants 05P15RFFC1 and 05P16PMF1, Romanian ANCSI/CAPACITATI Modul III Contract F04 and NUCLEU Project Contract PN 2018, Helmholtz-Alliance EMMI, HGS-HiRe.
Strategic university co-operation with: Frankfurt-M

Status on the CBM Time Of Flight system

I. Deppner[1], N. Herrmann[1], the CBM_TOF working group

[1]University of Heidelberg

We can look back, again, on a very successful year 2017. For the first time a trigger less readout system using close to final electronic components was operated successfully in the beamtime at SPS as well as in the cosmic setup in Heidelberg. Results concerning efficiency, time resolution and cluster size obtained in many beamtimes demonstrate that the counter development is far progressed and therefore in a very satisfactory situation. Along this line the mass production for the MRPC3a and MRPC3b counters [1] (foreseen for the FAIR phase 0 project at STAR and mCBM) started after the review readiness report in March 2017.

The main tasks for TOF in the last year were the following:

1) analysis of the data taken during the beamtime at ELBE in 2017 and at SPS in Nov. 2016,
2) operation of a free streaming cosmic stand in Heidelberg,
3) mass production of MRPC3a and MRPC3b counters for the FAIR Phase 0 projects at STAR and mCBM,
4) installation and conditioning of one eTOF sector in the STAR experiment at BNL.

Beamtimes are essential for testing high rate counters. At ELBE a mono-energetic single electrons beam of 30 MeV with pulse duration of 5 ps and a flux of $\leq$ 500 kHz/cm^2 is well suited to test the rate capability of single cell counters like the BFTC prototypes (active area is 4 cm^2) with ceramic resistive electrodes. However, since the beam has a diameter of only about 10 cm^2 only the spot response of counters larger than a few cm^2 can be tested. During the last year a beamtime at ELBE was carried out with the BFTC prototypes and results are reported in [2]. In order to achieve a full illumination on counters bigger than a few cm^2, beams with heavy ions impinging on lead targets like executed at CERN SPS is mandatory. The beamtime setup in Nov. 2016 (conf. Fig. 1), described in [3], consisted of about 500 read out channels distributed over 10 timing counters (including 2 layers of ceramic MRPCs) and one Bakelite resistive plate counter for the MUCH system from our Indian colleagues. For the first time a free streaming readout system was operated successfully and even synchronization with 2 GEM detectors (for the MUCH-subsystem) using FEBs with nXYTER (Rev-F) [4] could be demonstrated. During this campaign a Pb beam with an momentum of 156 AGeV/c was impinging on a 4 mm Pb target leading to high multiplicity events which are substantial to test the detector response under load. Occupancies higher than 50 % were reached. However, particle fluxes (measured by a plastic scintillator) above 1.5 kHz/cm^2 could not be reached even after adding 10 cm of iron to the target. As in the SPS beamtime in Nov. 2015 the radiation protection alarm was triggered and a reduction of beam intensity

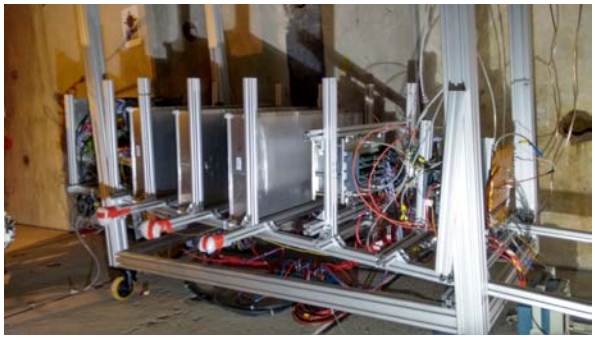

Figure 1: Photography of the CERN November 2016 setup. The beam enters the setup from the right side. The counters are arranged below the beam with an angle of 7◦.

was needed in order to continue the measurements. In conclusion the H4 beam line at SPS is not suited to deliver the anticipated rates for the inner part of the CBM TOF wall. Currently such high rates will only become accessible at the upcoming mCBM beamtimes at SIS 18 which shows the immense importance of this FAIR Phase 0 project not only in terms of DAQ integration tests but also as a test facility for high rate detectors. Nevertheless, during the beamtime at SPS more than 100 useful runs were taken which are right now still being analysed. First results for the MRPC1/2 prototypes [1] are presented in [5]. In order to adapt the MRPC1/2 prototypes to the front-end electronic and to minimize channel costs a redesign in the readout electrodes is currently ongoing where the number of channels is reduced from 40 to 32. The mechanical design for the inner TOF wall where these counters will be located is ongoing as well [6].

Equally important are counter tests with cosmic particles that have the advantage of being constantly available. A test stand for cosmics (see Fig. 2) was operated at Heidelberg during almost the full year. Per day about 100000 good tracks (in the acceptance of all counters) can be recorded and multi-dimensional analysis can be performed. On the left side of figure 3 an event with 2 tracks is shown that had hits in all 6 stations. Comparing 5 hit and 6 hit tracks, the efficiency as function of position in X and Y can be measured (see right plot in Fig. 3). Similar figures can be obtained for time resolution, cluster size, position resolution, time over threshold distributions and so on. In the cosmic setup counter time resolution of about 55 ps, X position resolution (across the strip) of about 2.5 mm and Y position resolution (along the strip) of about 5.5 mm was obtained. Beside resolution studies, the cosmic stand data also offer the opportunity to develop the software for calibration and reconstruction under clean conditions. In addition simulation with the same geometry can be performed and the counter response from realistic digitizer [7] as well as the analysis framework can be tested and compared to real data. However, this is not restricted only to cosmic data as shown in [8].

In the context of the CBM FAIR phase 0 programs for TOF the mass production of the MRPC3a and MRPC3b counter started in 2017. 73 MRPC3a counter with low

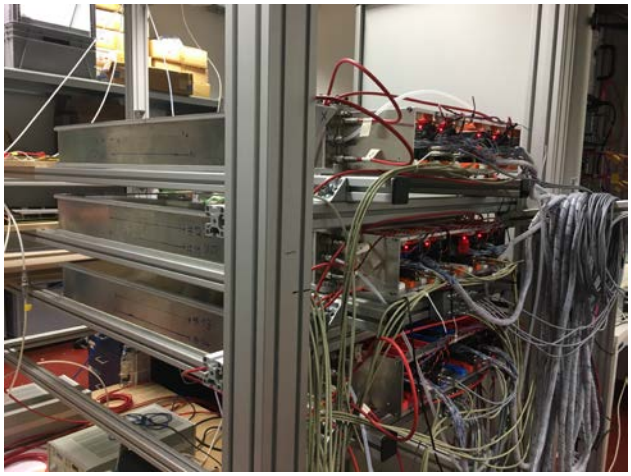

Figure 2: Photography of the Heidelberg cosmic setup. Three modules containing 2 counters each are placed on top of each other so that in total 6 counters can be tested simultaneously.

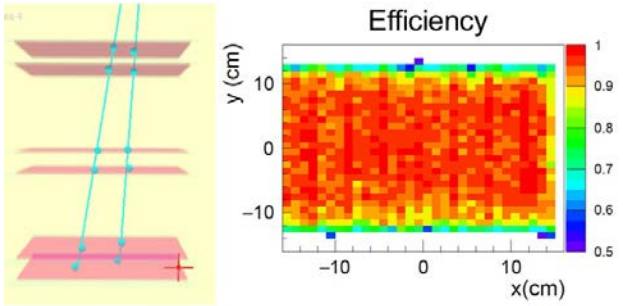

Figure 3: Left: cosmic setup with 6 MRPC stations. An event with 2 tracks with 6 hits each was found. Right: Efficiency of one MRPC as function of the X and Y coordinate.

resistive glass are produced at Nuctech in Beijing and most of them are tested and delivered to Heidelberg. The counter specs, the progress of the production, the test results as well as the QA procedure are described in [9]. It turned out that a conditioning time of about 120 hours is necessary in order to achieve stable operating conditions. 80 MRPC3b counter (float glass) are currently produced at USTC/Hefei. A short overview of the status and the QA procedure is given in [10]. The integration of the MRPC3a/b counters in modules will take place in Heidelberg. Currently 36 gas tight boxes for STAR and 5 boxes for mCBM are under construction in the mechanical workshop in Heidelberg. The module production for mCBM will be finished end of April while for STAR end of August. The plan is to test all modules extensively in the Heidelberg cosmic setup before the modules are delivered to GSI and to BNL.

Three modules for eTOF at STAR (see FAIR phase 0 program for TOF in [11] were produced last year, tested and shipped to Brookhaven National Laboratory. Figure 4 shows the three modules, forming one sector, mounted in the 6 o'clock position of the east-side end-cap of the magnet. The chambers are controlled remotely from Germany. Be- fore the RUN18 starts, cosmic data with the full STAR apparatus are taken and the data from eTOF are integrated in the data stream of STAR.

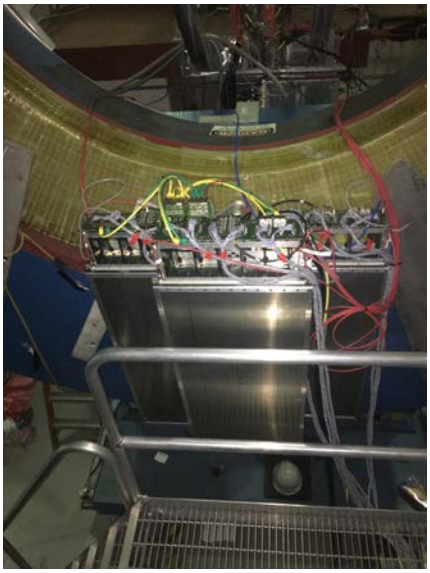

Figure 4: Sector consisting of 3 CBM-TOF modules moun- ted on the east pole tip of the STAR experiment.

This report is also part of the CBM Progress Report 2017 (doi:10.15120/GSI-2018-00485)

References

[1] N. Herrmann et al. "CBM-TOF Technical Design Report", http://repository.gsi.de/record/109024/files/, October 2014
[2] R. Sultanov et al., CBM Progress Report 2017 (2018)
[3] I. Deppner and N. Herrmann, CBM Progress Report 2016 (2017), S 124
[4] A. Kumar, CBM Progress Report 2016 (2017), S 88
[5] M. Petriș et al., CBM Progress Report 2017 (2018)
[6] L. Radulescu et al., CBM Progress Report 2017 (2018)
[7] C. Simon et al., CBM Progress Report 2017 (2018)
[8] Ph. Weidenkaff, CBM Progress Report 2017 (2018)
[9] P. Lyu et al., CBM Progress Report 2017 (2018)
[10] D. Hu et al., CBM Progress Report 2017 (2018)
[11] I. Deppner and N. Herrmann, CBM Progress Report 2017 (2018)

Experiment beamline: none
Experiment collaboration: CBM
Experiment proposal: none
Accelerator infrastructure: SIS100
PSP codes: 1.1.1.5
Grants: BNBF 05P15VHFC1
Strategic university co-operation with: Heidelberg

The CBM FAIR Phase 0 project - eTOF at STAR

I. Deppner[1], N. Herrmann[1], the CBM-TOF collaboration

[1]University of Heidelberg

The FAIR Phase 0 program of TOF comprises among other tasks the installation, commissioning and operation of 36 eTOF-modules, using 108 CBM-TOF MRPC3a/b counters [1], during the beam energy scan campaign II (BESII) of the STAR experiment at BNL. The modules will be grouped in 12 sectors and will be attached on the east side pole tip of the magnet (conf. Fig 1). During the last year a substantial progress regarding this project was made.

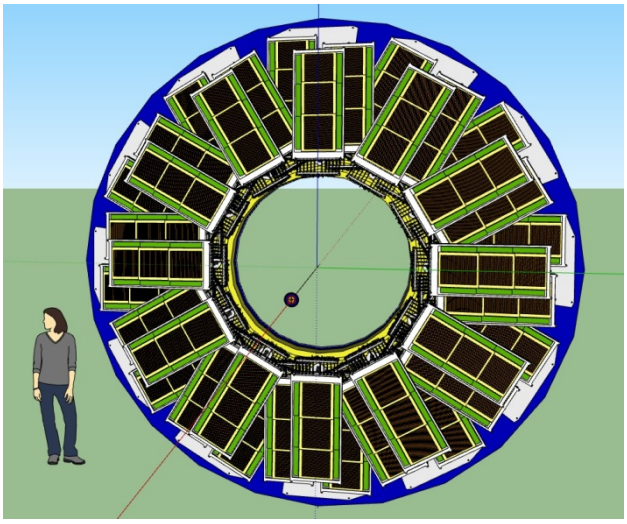

Figure 1: Conceptual design of the eTOF wall at STAR. The ”wheel” is composed of 36 module comprising 6912 readout channels.

The physical work of this project started with the installation of one module containing 2 MRPC3b counters at STAR in Jan. 2017 and operating it in the RUN17 (Mar. 17 - Jun. 17). The aim was to integrate our free streaming readout system in the trigger based readout system of STAR. It could be shown successfully that the first DAQ integration tests worked as expected (see last CBM Progress Report [2]). Currently software is developed in order to unpack the eTOF data and make them accessible to the STAR analysis framework. The test installation of the first module already delivered valuable information for a stable operation of our MRPC counters. After an accelerator intervention (un-planned beam loss event) one PADI FEE board stopped functioning pointing to the need for fast protection measures. After 2 month of operation both MRPC counters stopped working due to HV failure. This problem was analysed and cured by a modification in the design of the MRPC3b counter. These examples demonstrate the immense importance of the FAIR phase 0 programs in order to identify critical issues of the system under running conditions.

In the last year 3 modules for eTOF were produced. Two modules contain 3 MRPC3a counters each (with low resistive glass) manufactured at Nuctech in Beijing while 1 module is housing 3 MRPC3b counters build at USTC/Hefei. The module integration for the full wheel is carried out in Heidelberg. Figure 2 shows a photograph of the open module from the front side (left) and the back side (right). The 3 modules were shipped to BNL beginning of January 2018 and installed at the 6 o’clock position at the east pole tip (see Fig. 3). The readout system consists of the PADIX boards (inside the module box), a feed-through PCB, the TDC board with the GET4 V2.0 chip, a back-plane board distributing the power and the clock to the FEE cards, 5 AFCK boards sitting in a µTCA crate at 8 m distance from the modules and a FLIB board sitting in a rack mount PC located in the DAQ room about 50 m from the setup. The current connection between the back-plane board and the AFCK is copper cable (twisted pair) and will be re- placed with optical fiber after the RUN18. Then also the GBTx chip, sitting on the back-plane board, will be included in the readout chain. The connection between AFCK and FLIB is optical fiber.

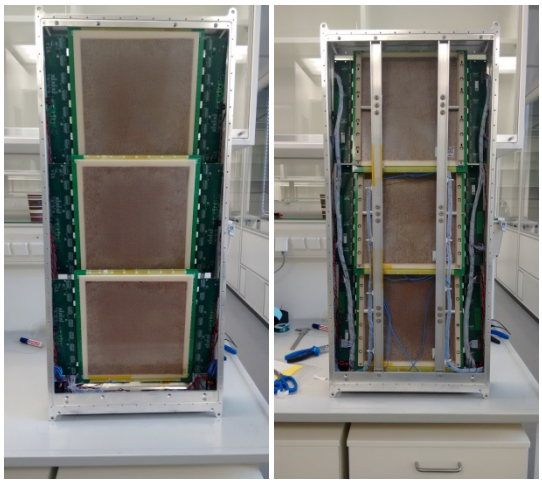

Figure 2: Open eTOF module - left: front side, right: back side.

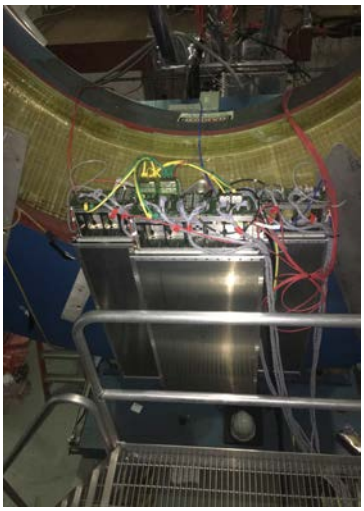

Figure 3: One sector mounted on the inner side of the pole tip.

In the meanwhile both institutes from China continued the mass production of the counters for the full eTOF wall (in total 150 counter). The production of the MRPC3a counters will be finished in March 2018 and 53 aut of 73 counters are shipped to Heidelberg. 25 of the MRPCa counters are devoted to the mCBM project. Figure 4 shows the production of MRPC3a counters in the clean room at Nuctech/Beijing. The clean room level is 100k. The production of the MRPC3b counter will be finished in July 2018. 5 counters are shipped to Heidelberg and integrated in the cosmic setup. The progress of the mass production as well as the QA procedure are summarized in [3, 4].

Figure 4: Mass production of MRPC3a counter in the clean room.

In order to coordinate and to discuss the progress as well as the open issues on the project two CBM-STAR meetings where organized during the last year. The first meeting took place at Darmstadt while the second meeting was carried out at Wuhan. Many fruitful discussion and solutions arises during these meetings. One example is the implementation of the eTOF geometry in the STAR simulation frame work (see Fig. 5).

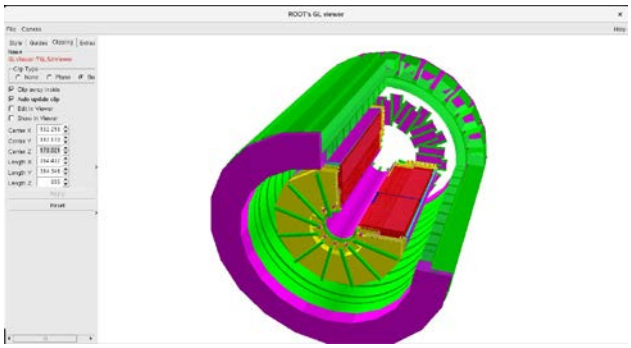

Figure 5: eTOF geometry included in the STAR simulation frame work.

The time line of the eTOF project is:
1) Jan 2018 - shipping and installation of one sector
2) Mar. - June 2018 - 2nd system integration test with one sector by participating in the Run18 beam time in STAR,
3) Mar. - Oct 2018 - Production and testing of 36 modules in Heidelberg
4) Sep 2018 - shipping of all 36 modules to BNL
5) Oct. - Feb. 2018 - Installation and commissioning of the eTOF syatem
6) 2019/2020 - Running in the BES II campaign
7) Summer 2021 - Decommissioning and shipping of all modules including infrastructure to FAIR

This report is also part of the CBM Progress Report 2017 (doi:10.15120/GSI-2018-00485)

References

[1] N. Herrmann et al. “CBM-TOF Technical Design Report”, http://repository.gsi.de/record/109024/files/, October 2014
[2] I. Deppner et al., TOF Summary, CBM Progress Report 2016 (2017)
[3] P. Lyu, CBM Progress Report 2017 (2018)
[4] D. Hu et al., CBM Progress Report 2017 (2018)

Experiment beamline: none
Experiment collaboration: CBM
Experiment proposal: none
Accelerator infrastructure: BNL-RHIC
PSP codes: 1.1.1.5
Grants: BNBF 05P15VHFC1
Strategic university co-operation with: Heidelberg

Development of muon detection system (MUCH) for the CBM experiment at FAIR

S. Chattopadhyay[1], A.K. Dubey[1], Z. Ahammed[1], J. Saini[1], P. Bhaduri[1], E. Nandy[1],V. Negi[1], M. Mandal[1],A. Kumar[1],C. Ghosh[1],S. Prasad[2], S. Biswas[2], S. Das[2], D. Emschermann[3], C. Schmidt[3], P. A. Loizeau[3], A. Senger[3],O. Singh[4], the CBM collaboration, and the FAIR@GSI division

[1]VECC, Kolkata, India; [2]Bose Institute, Kolkata, India; [3]GSI, Darmstadt, Germany,
[4]Aligarh Muslim University, Aligarh, India

The SIS-100 version of MUCH consists of five absorber segments with 4 detector stations sandwiched between them. While the first absorber is made of graphite, other absorbers are of iron. A gap of 10 cm houses the detector stations having 3 layers each consisting of varying number of chambers. The first and the second stations use GEM chambers to handle a hit rate of more than 400 KHz/cm^2. As the particle rate at the 3rd and 4th stations are considerably lower (maximum 5 KHz/cm^2 in Au+Au collisions at 10 AGeV), different technologies are being explored like high-rate RPC or straw tube chambers.

Two chambers fit to be placed in the 1st station are built at VECC-Kolkata and ready to be installed in the mini-CBM scheduled to take data in October 2018. The chambers (Fig. 1) use GEM foils from CERN custom-built for our configuration. Major features implemented in these chambers are (a) NS-2 technique for glue-less stretching (b) drift planes with opto-couplers connected to the HV line of each segment providing with a possibility of isolating the segment in case of any spark. This feature enables to use high-voltage segmentations using resistive chains thereby reducing the total cost of HV supply by a factor of 24 (the number of segments in each foil).

The readout planes of the chambers are having projective pads of varying sizes. Each pad covers 1 Degree in azimuth and equivalent radial distance. The chambers have been tested successfully with radioactive source (Fe-55, Sr-90) and ready to be installed in mini-CBM. A 1 cm thick Aluminium plate has been used to support the chamber and channels made inside the plate is being used for water-cooling. This setup has been tested to take data with Pb beam at SPS in November 2016.

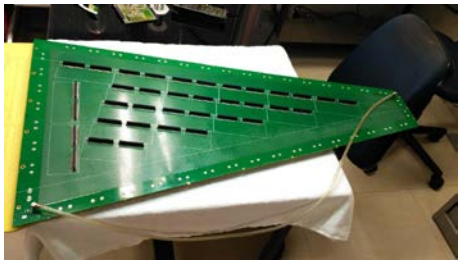

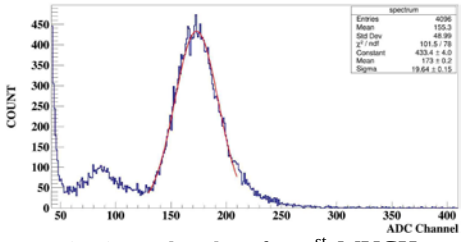

Fig.1 : (top) A chamber for 1st MUCH station (bottom) Fe-55 spectra

A low voltage distribution box (LVDB) has been developed to distribute LVs to the FEE boards. A FPGA-based system has been developed to control the operation of LVDB. A similar system has also been developed for the HV control. All components being used in the detector and supply systems have been tested with neutron and gamma sources to withstand a dose that is about a factor of two higher than estimated by FLUKA.

The MUCH system is being simulated using CBM-ROOT framework for measurement of LMVM and charmonia. The results obtained earlier have been found not to deteorirate using the most realistic geometry of the setup.

An ASIC called STS/MUCHXYTER have been developed for the MUCH readout and the version presently available has been connected to a GEM chamber for taking data with Sr-90 source. Even though the calibration is under progress, the readout shows clear source spot on the detector.

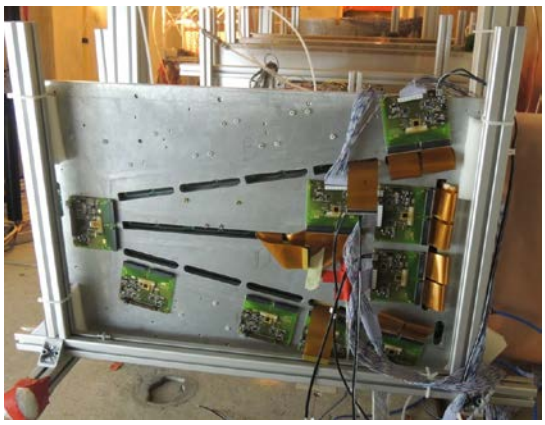

Fig.2: Al-plate for support and cooling of the GEM chambers. FEE boards are connected using small cables.

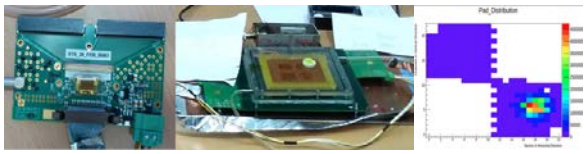

Fig.3: (left) STS-MUCHXYTER ASIC connected to a GEM chamber (right) beam spot seen online

A significant progress has been made on the mechanics of the MUCH system. Two major mechanical systems are absorbers and superframe to hold MUCH. Designs are in advanced stages and discussions are in progress with the prospective manufacturers.

One open area is to find a suitable technology for the 3rd and 4th stations of MUCH. Given the performance reported by ALICE muon chambers, two ALICE-muon RPCs have been tested with cosmics and with NINO and PADI electronics to provide >95% efficiency with cosmic muons. MUCH simulations using RPCs in the 3rd and 4th stations show good performance.

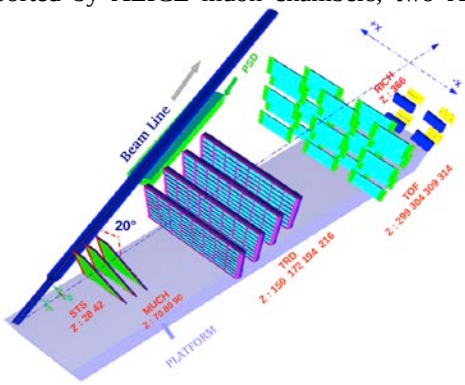

Fig. 4: 3 GEM chambers in miniCBM setup

Detailed setup has been developed to simulate the mini-iCBM setup including three GEM chambers. The digitization and formation of hits have been performed.

 DOI:10.15120/GR-2018-1

Preparation of a free-streaming DAQ system for mCBM@SIS18

D. Emschermann and C. Sturm for the CBM collaboration

The key objective of the Compressed Baryonic Matter experiment (CBM) at FAIR is to investigate the QCD phase diagram in the region of the highest net-baryon-densities by measuring nucleus-nucleus collisions. As a fixed-target experiment, CBM is consequently designed to cope with unprecedented collision rates up to 10 MHz which will allow studying extremely rare probes with high precision. To achieve the high rate capability, CBM will be equipped with fast and radiation hard detectors readout by a free-streaming data acquisition system transporting data with up to 1 TB/s to a large scale computer farm providing a first level event selection.

With mCBM@SIS18 we are presently constructing a CBM full-system test-setup at the GSI/FAIR host lab to study, commission and test the complex interplay of the different detector systems with the free-streaming data acquisition and the fast online event reconstruction and selection under realistic experiment conditions.

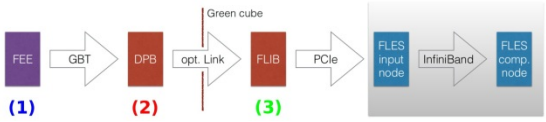

Figure 1: mCBM readout chain for the startup phase, based on DPB and FLIB. The mCBM subsystems are equipped with individual front-end electronics FEE (1). These front-ends are interfaced by the GBTx ASIC, which forwards the detector data via optical GBT link. All GBT links are received by the DBP layer located at 50 m distance in the DAQ container (2). The DPB is a FPGA based board which allows for subsystem specific pre-processing of the arriving data stream. A long optical link connects the DPB output to the FLIB board installed in the FLES input node in the Green IT Cube (3).

The detector stations will be equipped with final readout electronics containing ultra-fast and radiation-tolerant ASICs as front-end chips followed by CERN GBTx-based radiation-tolerant data aggregation units. Further down-stream, the data streams are handled by Data Processing Boards (DPB) containing powerful FPGAs and are forwarded via FLES Input Boards (FLIB), a PCIe based FPGA board, to a large-scale computer farm, the First-Level Event Selector (mFLES), which will perform on-line track and event reconstruction and selection, see Fig. 1.

The CBM detector front-ends are time-synchronized to the nanosecond level by the Timing and Fast Control (TFC) system. The detector front-end digitizes signals above threshold and assigns time stamps to hits. This data is then forwarded via an electrical connection to the GBTx readout board, where the electrical signals acquired through a large number of e-links are converted and merged into an optical GBT link operating at 4.48 Gbit/s. These GBT links are the detector interface to the Data AcQuisition (DAQ) chain.

On the road towards the full CBM DAQ system the mCBM DAQ system will be deployed in two phases. During phase I, the GBTx-based subsystems (mSTS, mMUCH, mTRD and mTOF) will be read out using already available readout chains based on existing prototype implementations of DPB and FLIB, see Fig. 1. As current prototype hardware, an AMC FMC Carrier Kintex (AFCK) board [1] is used for the DPB, a HiTech Global HTG-K700 PCIe board for the FLIB. Both boards are based on a Xilinx Kintex-7 FPGA. In phase II, DPB and FLIB will be replaced by a prototype of the Common Readout Interface (CRI) (see Fig. 2) in the FLES input stage, as it is foreseen for the CBM experiment. In addition, the mCBM subsystems (mRICH, mPSD) readout with FPGA TDCs chains will be added to the DAQ setup in 2019.

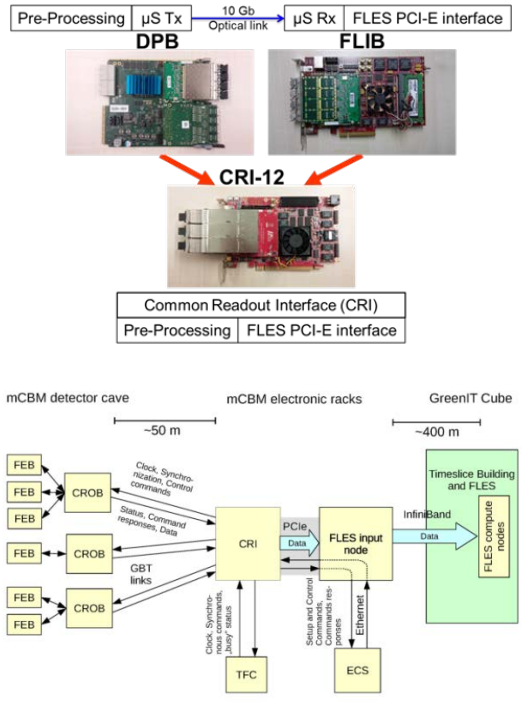

Figure 2: Upgrade of the mCBM DAQ in 2019, from two chained Kintex-7 devices to a single Ultrascale+ FPGA (top panel). This results to the final CBM DAQ scheme (bottom panel) [2].

References

[1] D. Hutter, J. de Cuveland, and V. Lindenstruth, Preparations for the mCBM FLES Setup, CBM Progress Report 2017, doi: 10.15120/GSI-2018-00485

[2] W.M. Zabołotny et al., Selection of hardware platform for CBM Common Readout Interface, Photonics Applications in Astronomy, Communications, Industry, and High Energy Physics Experiments 2017; 10445 (2017) 49, doi: 10.1117/12.2280938

Status of the CBM physics performance studies

I. Selyuzhenkov[1,2], I. Kres[3], C. Pauly[3], K.H. Kampert[3], M. Zyzak[1], I. Kisel[4], P. Kisel[1,5], I. Vassiliev[1], V. Klochkov[1,6], A. Senger[1], E. Bechtel[6], C. Blume[1,6], S. Glaessel[6], J. Book[6], H. Schuldes[6], M. Teklishyn[7], and H. Malygina[1] for the CBM collaboration

[1]GSI, Darmstadt, Germany; [2]MEPhI, Moscow, Russia; [3]Bergische Universität Wuppertal(BUW); [4]Frankfurt Institute for Advanced Studies(FIAS), Frankfurt, Germany; [5]JINR, Dubna, Russia; [6]Goethe-Universität Frankfurt, Frankfurt, Germany; [7]FAIR, Darmstadt, Germany

Introduction

The CBM experiment is designed to study the QCD phase diagram at high net-baryon densities and moderate temperatures with heavy-ion collisions at the high interaction rates. In this report we highlight the activities of the CBM Collaboration related to the physics performance studies.

π^0 reconstruction via double conversion

The produced heavy particles containing charm quarks, like J/ψ, and also rare vector mesons ω, ρ, φ can be detected via their leptonic decay ω/ρ/φ → e^+e^-. As leptons are insensitive to hadronic interaction with the dense medium, their leptonic decays offer a possibility to look into the early, dense phase of the fireball evolution. Due to their comparatively small production cross section, together with small branching ratio (BR) into e^+e^- a precise understanding of background is needed. A major source of background stems from decay of neutral pions into π^0 → γ+γ (BR 98.8%), aand π^0-Dalitz decays π^0 → e^++e^-+γ (BR 1.1%). Instead of measuring directly photons by using an electromagnetic calorimeter, the CBM-RICH detector is able to measure photons indirectly by detecting e^+e^--pairs stemming from conversion γ → e^+e^- in the target or in the material of the detectors. Two such reconstructed photons are then further combined to form a π^0.

The reconstruction efficiency for pions via double conversion is rather low (~ 10^{-4}), mainly due to the low conversion probability of the two photons. A precise acceptance and efficiency correction is required in order to quantitatively describe the π^0 background in dilepton studies. Two statistically independent Monte Carlo samples (each consists of 5 × 10^6 UrQMD events of central Au+Au collisions at 8 AGeV beam energy) are used to evaluate the analysis procedure. The first sample is used to derive a multi-dimensional (as a function of p_T and rapidity) acceptance and efficiency correction matrix. Using the fixed correction matrix, the data from the independent second sample (and also others in future) are analyzed. In Fig. 1 one can see the comparison between all generated (left panel) and reconstructed (middle panel) number of π^0 from the first simulated sample. The right plot shows their ratio, which determines the correction factors. These factors will be used for the realistic π^0 estimation from the second simulated sample. As can be seen from the different colors on the right plot of the Fig. 1, correction factors for different rapidity-p_T bins differ, therefore, the double conversion analysis has to be done for each rapidity-p_T bin separately, adding corresponding correction factors. Summing up all numbers of π^0 after the correction gives us the proper number of generated pions in the available acceptance.

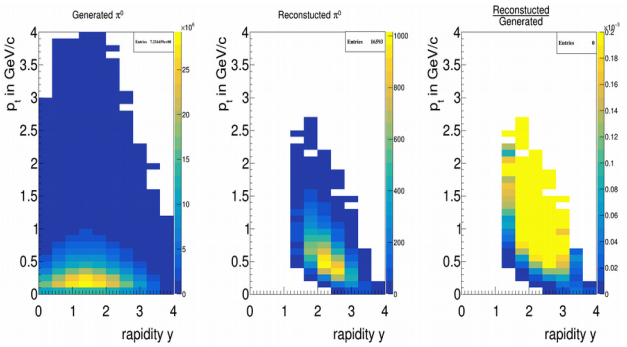

Figure 1: Phase-space coverage of all generated π^0 on the left plot, all reconstructed π^0 via conversion method on the middle plot, together with the their ratio on the right plot.

The corrected number of pions can be used for the temperature estimation of the emitting source. After summing up over rapidity to form 1-dimensional p_T distribution one can fit the resulting distribution and extract the corresponding temperature. In Fig. 2 one can see the comparison between reconstructed and generated p_T distributions together with the temperature fits.

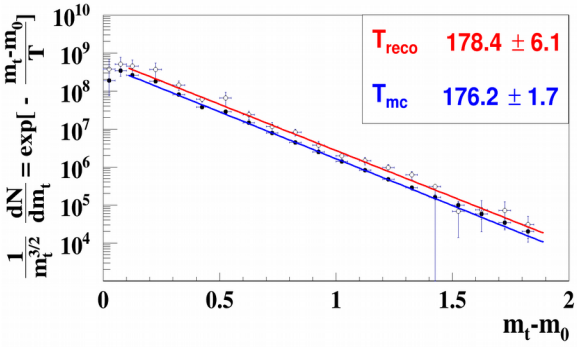

Figure 2: 1-dimensional p_T distributions of reconstructed π^0 after corrections (open circles) and simulated π^0.

Reconstruction of short-lived particles

The main goal of the short-lived particle analysis is to extract physics observables that characterize the system produced in a heavy-ion collision. One of such observables are particle yields as a function of momentum, rapidity, transverse mass, etc. In order to reconstruct short-lived particle spectra two methods were implemented in the KF Particle Finder package: side bands and background fit methods. The side bands method assumes that the back-

 DOI:10.15120/GR-2018-1

ground under the mass peak and around it has the same shape for all physics parameters. Under such assumption two kinds of spectra are collected for each parameter (p, rapidity, p_T, m_T) as well as two dimensional y-p_T and y-m_T spectra: signal+background within ±3σ of the peak and background in the region (3-6)σ around the peak. Then the background is normalized with respect to the integral of the background function in the region of ±3σ around the peak and subtracted from the signal+background spectra, that gives a reconstructed signal spectra.

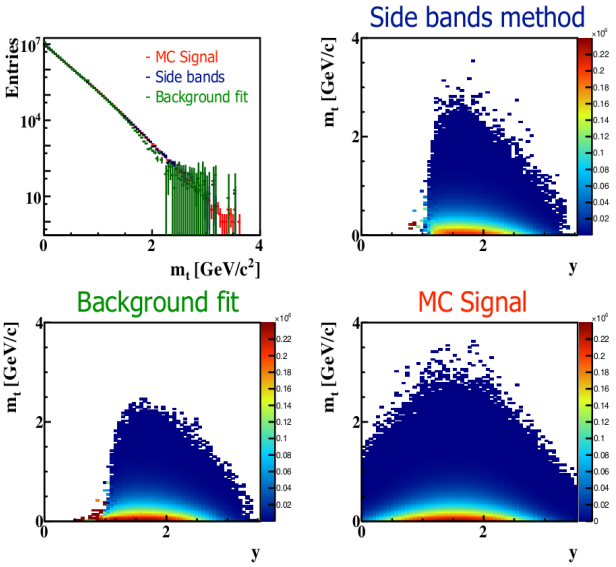

Figure 3: Efficiency corrected spectra of $K_s^0 \rightarrow \pi^+\pi^-$ decay as a function of m_t and y-m_t obtained by the side bands and background fit methods in comparison with the simulated Monte Carlo signal from 5M central Au+Au UrQMD collisions at 10 AGeV.

The second method which uses the background fit is implemented as follows: three dimensional histograms y-p_T -M and y-m_T-M are collected, where M is mass. Then the mass spectrum in each y-p_T or y-m_T bin is fitted with a signal+background function and the integral of the signal function provides the number of short-lived particles with given y and p_T or y and m_T respectively. The obtained number is filled to the corresponding bin of the signal spectra. Tools for collection of the efficiency plots were added to KF Particle Finder, that allow to reconstruct distributions of particles produced in the collision. Efficiency corrected m_T and y-m_T spectra obtained with both methods are shown in Fig. 3 for $K_s^0 \rightarrow \pi^+\pi^-$ decay in 5M central Au+Au UrQMD events at 10 AGeV. Reconstructed spectra are in a good agreement with each other and with the simulated Monte Carlo spectra.
The obtained m_T spectra can be further analyzed, for instance, in different rapidity bins, as it is shown in Fig. 4 - both reconstructed and simulated distributions are fitted with exponential functions, thus, providing the slope parameter. Under assumption, that produced particles are thermally distributed, the temperature can be extracted from the slope parameter.

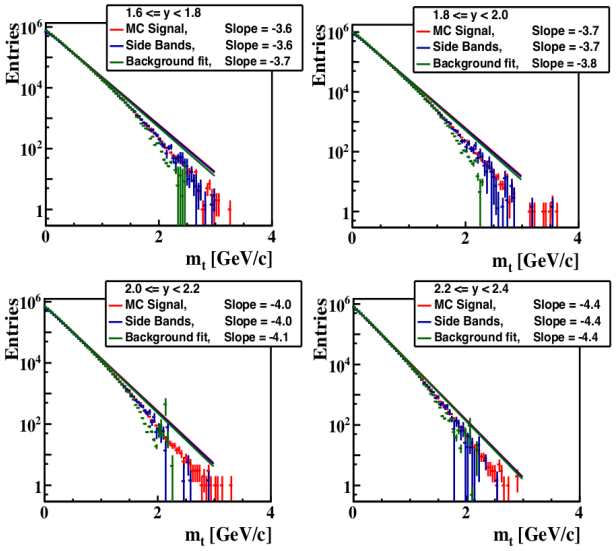

Figure 4: Reconstructed m_T signal in comparison to the simulated MC signal in different rapidity bins at an example of $K_s^0 \rightarrow \pi^+\pi^-$ obtained from 5M central Au+Au collisions.

Performance for directed flow measurement

The measurement of the anisotropic transverse flow is an important part of the CBM physics program. Due to the interaction among particles produced in a heavy-ion collision, the initial spatial asymmetry in the overlap region of the collision leads to the asymmetry in the direction of the particle's transverse momenta. This asymmetry can be measured via azimuthal distributions of produced particles with respect to the initial symmetry plane (reaction plane, RP) spanned by the impact parameter and the beam direction.
A sample of 5 million Au+Au collisions with beam momentum of 10 AGeV simulated with UrQMD event generator was used. Charge particles tracks were reconstructed using the Silicon Tracking System (STS) and Micro-Vertex Detector (MVD). The Projectile Spectator Detector (PSD) modules were grouped for analysis into three sets: central (PSD1), middle (PSD2) and outer (PSD3). Particle identification was done using Monte-Carlo information. Centrality determination was based on STS track multiplicity. The momentum asymmetry is quantified by constructing two-dimensional vectors q_n determined event-by-event from the STS tracks and calculated for three PSD module groups. Introducing a second harmonic vector helps to reduce non-flow correlations, such as contribution due to total momentum conservation. Imperfect acceptance and efficiency of the detector are biasing the azimuthal angle distribution of measured particles. A correction procedure for the q_n and Q vectors is implemented as a part of the QnCorrections framework.
Extracted values of the directed flow as a function of rapidity for negatively charged pions with reaction plane estimated from three different PSD subevents are shown in Fig. 5.

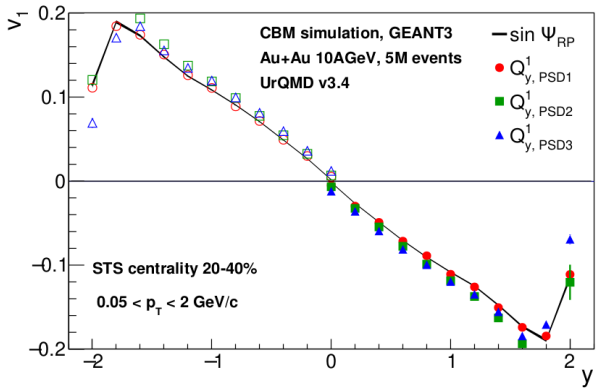

Figure 5: Directed flow of negatively charged pions for the 20-40% centrality class obtained using the y components of the PSD Q-vectors. Shaded area corresponds to v_1 calculated using MC-true reaction plane.

Di-muon measurement at low, intermediate and high invariant masses

The design of the CBM MUCH system consists of one absorber made of 60 cm carbon with additional Pb shielding around the beam pipe (5.7 degrees) and iron absorbers with thickness 20, 20, and 30 cm. Triplets of tracking detectors are mounted behind each absorber layer. Each tracking station behind the first and second absorber layer consists of 3 GEM detectors with high granularity in order to cope with the high particle density in these stations. The particle density behind the third and the fourth absorber is already significantly decreased, so that detectors with lower granularity could be used in order to reduce the number of channels.

The setup discussed above was optimized for measurements of the dimuon spectra in low invariant mass region. The Time-of-Flight (ToF) detector located 8 m downstream the target is used to suppress the background of protons and kaons. Figure 6 depicts the mass distributions for muons from ω (top) and for background (bottom) which are calculated using the time information. These simulations were performed for central Au+Au collisions at 8 AGeV generated with the UrQMD code assuming radial segmentation of 1 degree in stations 1 and 2, and 2 degrees in stations 3 and 4. The acceptance of the setup as a function of transverse momentum and rapidity is illustrated in the upper panel of Fig. 7.

An additional iron absorber of 1 m thickness behind the last detector station is required for measurements of the intermediate and high invariant mass regions. This study is devoted the investigation of the possibility to measure muon pairs over the full invariant mass spectrum. The simulations are based on the absorber system including the last absorber of 1 m thickness. In this case, the time measurements using the ToF detector are possible only for long tracks passing through all absorbers. Therefore, the soft muons are absorbed, and the acceptance of the reconstructed muons pairs will be shifted to forward rapidities (see central panel in Fig. 7). On the other hand, the signal-to-background ratio is very good, exceeding a value of 2 for omega mesons (see black histogram in Fig. 8). A possibility to shift the acceptance for dimuon signals back to midrapidity is to combine different types of tracks, for example long tracks with ToF information, and short tracks without ToF information. The acceptance for long-short and long-long combinations is shown in the lower panel of Fig. 7. The corresponding signal-to-background ratio is represented by the green histogram in Fig. 8.

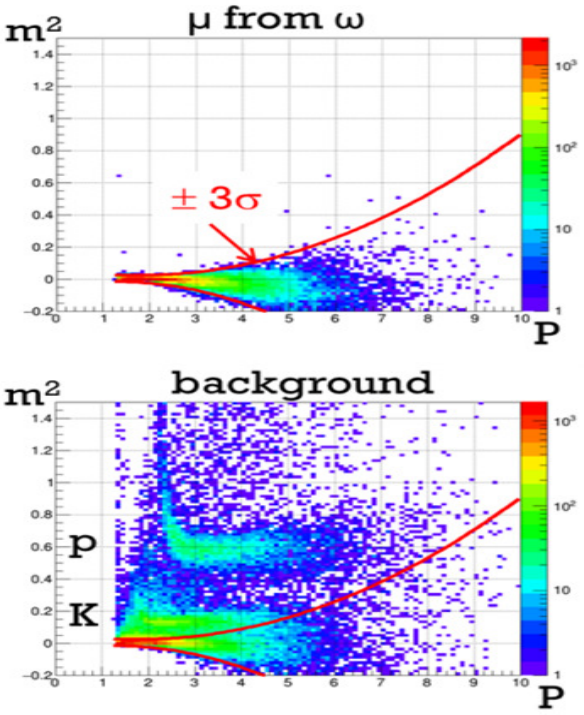

Figure 6: Mass squared versus momentum of muons distributions from omega meson decays (upper panel) and for protons, kaons and pions (lower panel) using ToF measurements. The red lines represent a 3 sigma selection of muon candidates by ToF.

In order to shift the acceptance further towards mid-rapidity, and simultaneously increase the signal-to-background ratio, one can consider an additional time-of-flight measurement in front of the last 1 m thick absorber. In this case, the contribution of short tracks to the background can be reduced, and all track combinations for muon pairs can be used: long-long, short-long, and short-short. Simulations have been performed with a ToF detector in station with a time resolution of 80, 200, 500 and 800 ps. Assuming a time resolution of 80 ps, the acceptance corresponds to the upper panel in Fig. 7, and the resulting signal-to-background ratio is represented by the red histogram in Fig. 8. For a much worse time resolution of 800 ps the signal-to-background ratio decreases by 35% only. When using only long-long and long-short track combinations together with the time measurement in station 4, the signal-to-background ratio improves further.

 DOI:10.15120/GR-2018-1

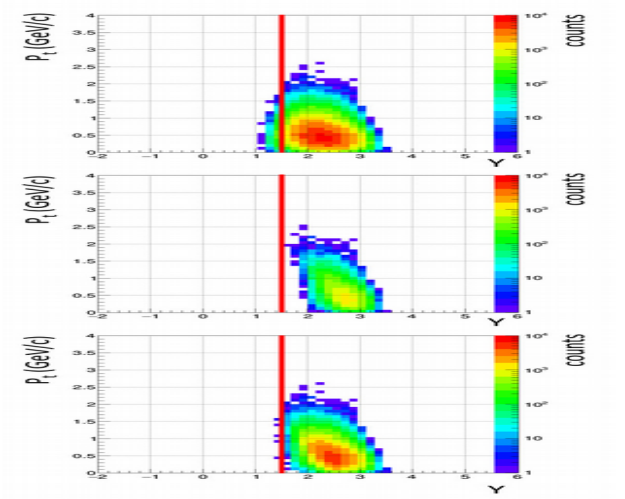

Figure 7: Acceptance for reconstructed muon pairs as a function of transverse momentum and rapidity. Upper panel: muon pairs from all muon track candidates. Middle panel: muon pairs from long tracks traversing 1 m iron absorber. Lower panel: muon pairs from short and long tracks. The red lines refer to mid-rapidity for 8 AGeV.

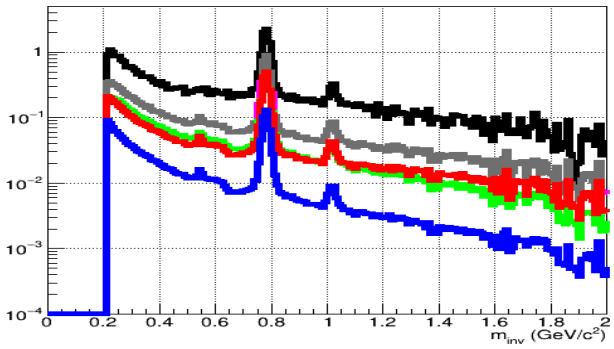

Figure 8: Signal-to-background ratio for muon pairs as a function of invariant mass for central Au+Au collisions at 8 AGeV. Black: muon pairs from long tracks with ToF information, Grey: muon pairs from long-long and long-short tracks, both with ToF information, Red: muon pairs from long-long, long-short, and short-short tracks, both with ToF information.

Dielectron measurements in Au+Au collisions

The measurement of dielectrons with sufficient signal-to-background ratio is essential for the CBM experiment. A good particle identification has to be provided in all momentum regions. For momenta below 6 GeV/c this can be done with the RICH detector. In the region of higher momenta the RICH loses its identification capabilities. The TRD can expand the particle identification and provide the necessary pion suppression to get access to the thermal radiation created in heavy-ion collisions.

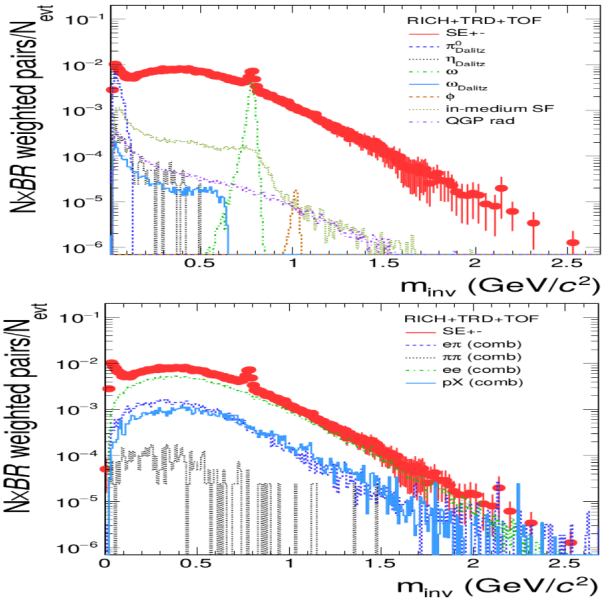

Figure 9: Invariant mass distribution for different unlike-sign pairs identified as electrons for central (10%) Au+Au collisions at 8 AGeV (red points), together with various signal channels (upper panel) and the combinatorial background contributions (lower panel). All contributions are weighted with their expected yield and branching ratio.

Figure 9 shows the invariant mass spectrum for different dielectron channels in the upper part. The simulation is done with 5 million Au+Au collisions at 8 AGeV beam energy for central (10%) events with the newest geometry of the TRD detector modules and four layers and a target thickness of 25 µm. A cocktail of low mass vector mesons (ρ, ω, ω dalitz and φ) as well as thermal radiation from the
hadronic and partonic medium is added via PLUTO generator. The electron identification for the RICH is done with the ANN output, tuned to a momentum independent efficiency of 90%, and for the TRD with the likelihood method tuned to 80% efficiency. The TOF identification uses β measurement to achieve an identification efficiency of ~ 90%. A p_T cut was used with a minimum of 0.2 GeV/c. The red points at the top panel of Fig. 9 show the total amount of reconstructed unlike-sign pairs which were identified as electrons. The signals of the in-medium and the QGP radiation are shown as violet and dark green dotted lines and can be accessed in the invariant mass range above 1 GeV/c^2 with a sufficient signal-to-background ratio. In the lower panel of Fig. 9 the corresponding background contributions are shown. The dotted green line presents the residual combinatorial dielectron pairs (e^+e^-) which are the most significant background contribution up to ~ 1.8 GeV/c^2. The other three lines consist of different hadronic combinations, which were misidentified as electrons but are strongly suppressed with respect to the e^+e^- component.

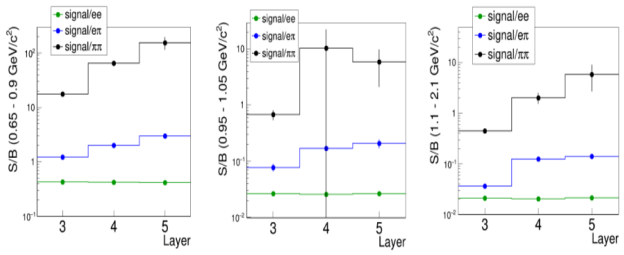

Figure 10: Total signal-to-background ratio in the range around the ω (0.65 − 0.9 GeV/c^2 - left), the φ (0.95 −1.05 GeV/c^2 - middle) and where the thermal radiation is expected to be dominant (1.1 − 2.1 GeV/c^2 - right).

To verify the best detector setup the simulation was also done for three and five TRD layers. Their performance can be quantified via the different signal-to-background ratios in the respective invariant mass regions as shown in Fig. 10. The four layer TRD setup shows a strong performance improvement in comparison to the three layer setup and provides sufficient identification for the requirements.

Hadron identification with the TRD

An important part of the CBM physics program is a high statistics measurement of double-Λ hypernuclei. Since up to now only very few double-Λ hypernuclei events have been identified, the measurement is considered to be a break-through in this field of physics. The Transition Radiation Detector (TRD) will significantly extend the number of hypernuclei states accessible within the program. For the identification of $^{6}_{\Lambda\Lambda}$He, which decays as $^{6}_{\Lambda\Lambda}$He → $^{5}_{\Lambda}$He+p+π and subsequently as $^{5}_{\Lambda}$He → ^{4}He+p+π , the separation of d and He is particularly important. The m/Z measurement of hadrons alone, as provided by the Time of Flight Detector (TOF), is not able to distinguish between the two different charge states. The TRD contributes to the separation of charged hadrons with a measurement of the specific energy loss. Fig. 11 shows how the identification of the light nuclei d and ^{4}He can be performed by combining TOF and TRD information.

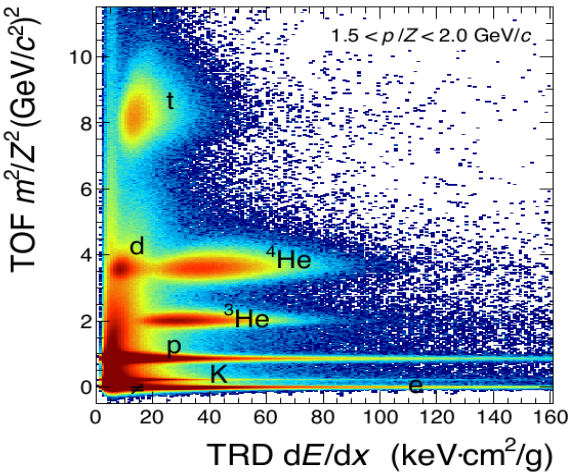

Figure 11: TOF versus TRD Mass squared distribution for 1.5 < *p/Z* < 2.0 GeV/c.

The distributions of the averaged energy loss signal *dE/dx* of d and ^{4}He, as reconstructed in the TRD for Au+Au collisions at 8 AGeV, are displayed in Fig. 12 for one momentum interval. A clear separation of d and ^{4}He is visible. The dE/dx distributions are fitted with a modified Gaussian, which includes the non-Gaussian tails of the distributions via the parameters α and β. Based on the corresponding energy loss resolution *σ(p/Z)/dE/dx(p/Z)*, the separation power can be determined for different particle species. The separation power for deuterons and ^{4}He for different detector geometries is shown in Fig. 13. A separation of d and ^{4}He on a level of σ ≥ 4 is achievable in the whole accessible momentum range with four TRD layers.

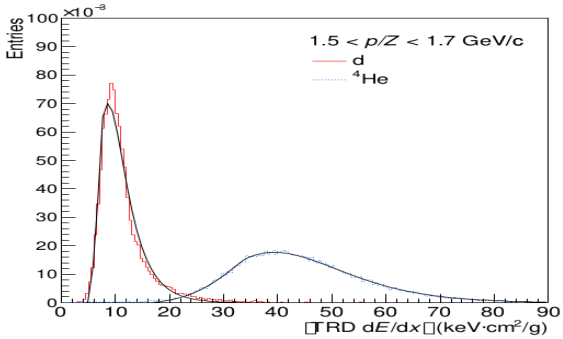

Figure 12: *dE/dx* distributions for d and ^{4}He, as reconstructed with the TRD, fitted with a modified Gaussian.

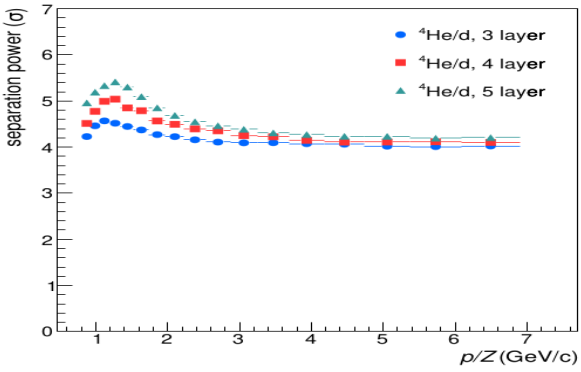

Figure 13: Separation power for d and ^{4}He as a function of momentum for setups with 3, 4 and 5 TRD layers.

Particle identification with the STS

Particle identification based on the energy loss in a thin absorber is a well-known technique in nuclear and particle physics. It can be naturally implemented in a tracking system by studying the energy loss Δ*E*/Δ*x* as function of the measured ratio of particle momentum and charge p/q. In the following we study the possibility of using the CBM-STS detector for particle identification in addition to the dedicated PID detectors (e.g., TOF). This way we expect to obtain a separation power for some particular cases such as low momentum particles not registered by the downstream detectors, decays inside the STS, and particles with the same m/Z ratio, e. g. ^{2}H and ^{4}He, which cannot be distinguished by means of a time-of-flight measurement alone. Since each track consists of several hits, each of which consists of two clusters, there are 2×N hits measurements of ΔE/Δx for a track. Each re-

 DOI:10.15120/GR-2018-1

constructed track has at least three hits in the STS. The chosen implementation for STS is based on the tracker geometry and readout electronics characteristics. The STS readout ASIC (STS-XYTER) has a dynamic range of 15 fC and a 5-bit flash ADC for each channel. These properties limit the implementation of the ΔE/Δx technique. If the charge in a given channel exceeds 15 fC (overflow), the energy loss measurement for the entire cluster (sum of all channels in the cluster) cannot be relied on.

For a proof of concept, we simulated 10^5 particles of various types (see Fig. 14) according to a thermal momentum distribution for Au+Au collisions at 10A GeV. A realistic detector response was involved in the simulation. An equivalent-noise charge of 1500e was used, which is 150−200% of the expected noise for a sensor connected to the readout electronics with a micro-cable; the threshold value was 3 × 1500 e = 4500e. Figure 1 shows that the energy loss measurement gives a reliable separation between single- and double-charged particles for the total momentum range, and separation between Hydrogen isotopes up to 2.5 GeV. The presence of clusters with overflow limits the application of the method in particular for heavy particles with low momentum. The efficiency is more than 99.99% for tritons and lighter particles, and 96.6% for the heaviest simulated particle ^{4}He (integrated over the whole momentum range). It is 100% for p > 2.5 GeV for all particles and drops for lower momenta.

The ΔE/Δx technique was tested on the example of ^{3}H reconstruction (see

Fig. 15). In this particular case it improves the signal-to-background ratio by a factor of 50 compared to using TOF alone for the identification of the decay products; the efficiency drops only by 0.3%. The method appears to be promising and shall be further developed for the implementation in the CBM software as one of the PID tools.

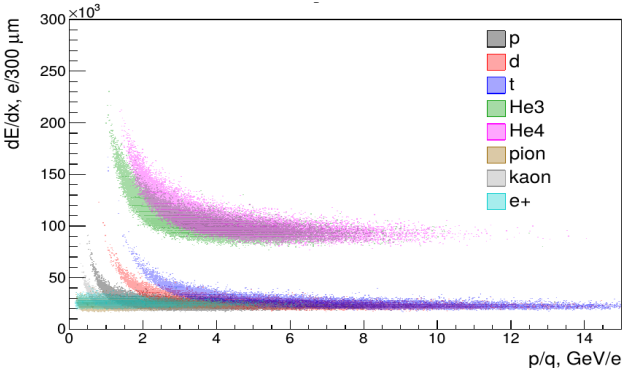

Figure 14: The reconstructed dE/dx normalized to the sensor thickness versus the reconstructed momentum-to-charge ratio from simulation of the CBM-STS.

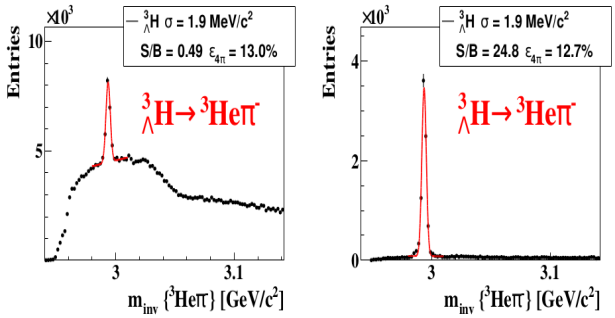

Figure 15: $^3_\Lambda$H reconstruction with TOF only (left) and with an additional PID from STS (right). 5×10^6 central Au+Au collisions at 10A GeV were simulated.

References

[1] [The CBM Collaboration], Chapter “Physics performance” in the CBM Progress Report 2017, DOI: 10.15120/GSI-2018-00485 (2018)

mCBM@SIS18 is on its way*

C. Sturm[1], D. Emschermann[1], J. de Cuveland[3], V. Friese[1], N. Herrmann[2], D. Hutter[3], P.-A. Loizeau[1], W. Niebur[1], A. Senger[1], F. Uhlig[1] , for the CBM collaboration

[1]GSI, Darmstadt, Germany; [2]Ruprecht-Karls-Universität Heidelberg, Germany, [3]Frankfurt Institute of Advanced Studies (FIAS), Frankfurt am Main, Germany.

The Compressed Baryonic Matter experiment (CBM) will explore the QCD phase diagram at the highest net-baryon densities by investigating nucleus-nucleus collisions in fixed-target mode at FAIR energies. The unique feature of CBM is its high-rate capability of up to 10^7 collisions per second, which will make it sensitive to extremely rare probes. In order to achieve these ambitious goals, CBM will employ fast and radiation-hard detectors as well as readout electronics. A novel, free-streaming data acquisition will be used, which aggregates the data sent by the self-triggered front-end electronics and pushes them to an online compute farm for data reconstruction and selection in real time.

By today, the design of the detector and electronics components for CBM is largely completed, and series production is going to start. The components were tested in the laboratory and in beam. Consequently, the next step is to test and optimize the operation of the full system of complex hard- and software components – from the detectors over the readout ASICs and the DAQ to on- and offline data processing and analysis – under realistic experiment conditions before the installation and commissioning of the full CBM detector setup. For this purpose we are presently installing a full-system test-setup for CBM at the GSI/FAIR host lab site under the name mCBM@SIS18 (”mini-CBM”, later shortened to mCBM). This test-setup will include detector modules from all CBM detector subsystems (MVD, STS, RICH, MUCH, TRD, TOF, ECAL and PSD see [1] - [6]) using prototypes or (pre-)series detector modules (mMVD, mSTS, mMUCH, mTRD, mTOF, mRICH, mECAL and mPSD).

Commissioning and running mCBM will complete our knowledge on proper functioning as well as on the performance of the CBM detector systems and their associated Front-End Electronics (FEE) before the final series production starts. The experiences gained during the complete mCBM campaign will significantly shorten the commissioning period for the full CBM experiment at SIS100.

Design of the test-setup

The mCBM test-setup will be positioned downstream a solid target under a polar angle of about 20° with respect to the primary beam, see Fig. 1 and 5. The present status of the mCBM engineering design is described in ref. [7]. mCBM does not comprise a magnetic field, and, therefore, will measure charged particles produced in nucleus-nucleus collisions traversing the detector stations following straight trajectories.

The tracking system comprises 2x STS (mSTS, see [8]), 3x MUCH (mMUCH) [9] and 4x TRD (mTRD) stations in total 9x tracking layers which provide redundant position information and allow to perform tracklet searches.

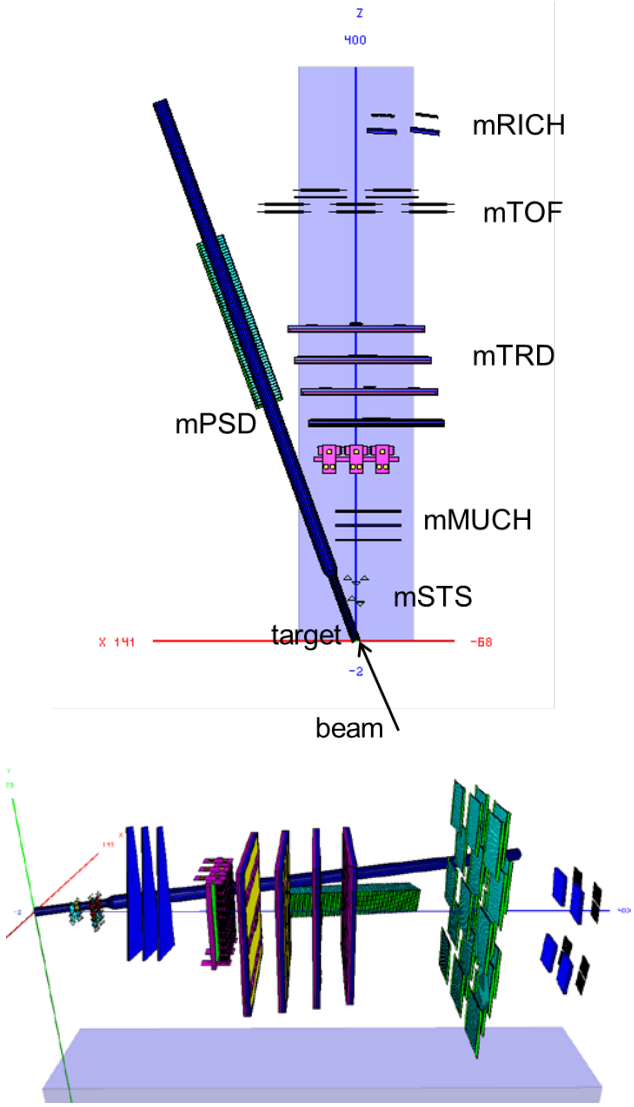

Figure 1: Top view (top panel) and side view (bottom panel) of the mCBM test setup (ROOT geometry) at the HTD cave. The detector stations are aligned at an emission angle of about θ_{lab}= 8° (beam pipe side, y = 0). Note, the GEM counters of the mMUCH subsystem are trapezoidal shaped (see lower panel), which is not visible in the top-view projection.

The setup will include a high-resolution time-of-flight system consisting of a fast and segmented diamond counter for time-zero (T_0) determination in front of the target as well as a TOF stop wall (mTOF) [10]. The mTOF detector modules are shown in Fig. 3 of [11]. An aerogel type RICH detector will be placed as the mRICH subsystem behind the mTOF detector and deliver a second measurement of the particle velocity in a selected ac-

 DOI:10.15120/GR-2018-1

ceptance window [12]. A small calorimeter (mECAL) will also be mounted behind the mTOF covering a reduced acceptance. Additionally, a PSD prototype-module (mPSD, see [13]) will be positioned directly under the beam pipe, 5° tilted relative to the beam axis while pointing to the target. In a later stage MVD stations (mMVD) will be added into the test-setup enabling a high-precision vertex reconstruction. However, the initial configuration of the mCBM test-setup is rather versatile and can be variably adapted according to the needs. Therefore, the detector stations are going to be mounted on sliders of a rail system on top of the mounting table.

The two mSTS stations and the 4^{th} layer of mTRD are centred in x and y. For tracks passing the active area of the mSTS, mMUCH, mTRD and mTOF subsystems the covered θ_{lab} range results to 8° – 32°. The overall acceptance is limited by the mSTS, which is located very close to the beam pipe [8] and cannot be moved further upstream.

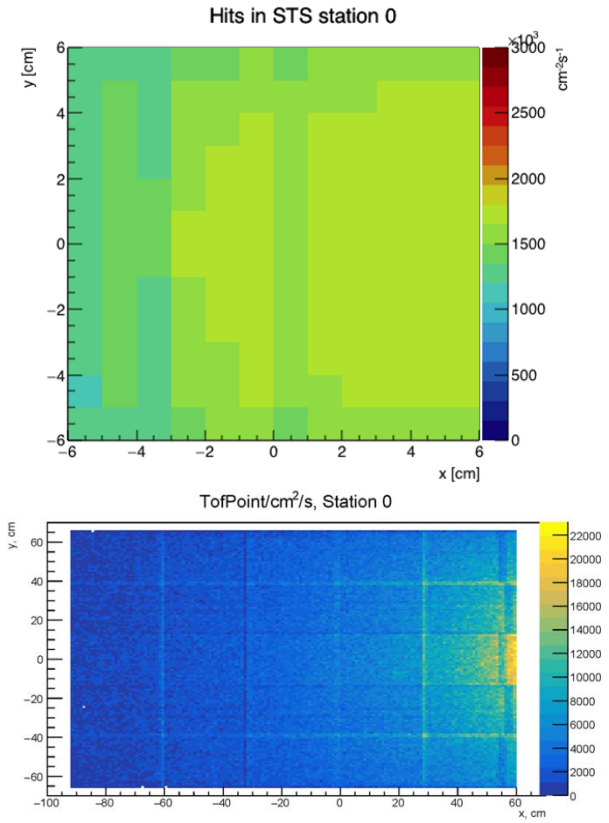

Figure 2: Hit rate within the first station of the mSTS (top panel) and of the mTOF (bottom panel). As input for the simulation, UrQMD events for minimum bias Au + Au col- lisions at 1.24 AGeV has been generated. δ-electrons have been taken into account.

Extensive Monte Carlo simulations have been performed to optimize the geometry of the setup. As input, events for minimum-bias Au+Au collisions at 1.24 AGeV have been generated with the UrQMD transport code. The complete mCBM geometry as shown in Fig. 1 has been implemented in CbmRoot and used for GEANT3 particle transport simulations taking δ-electrons into account. Within the mCBM acceptance an average charged-track-multiplicity yields to about 5 in minimum-bias and about 30 in central Au+Au collisions. In Fig. 2 hit rates normalized to 10^7 collisions per second (10^8 Au ions/s on a 10% interaction Au-target) are shown which have been obtained inside the first mSTS station (top panel) as well as in the mTOF stop wall (bottom panel). As shown, the hit rates result up to 1.8 MHz/cm^2 in the first mSTS station (mSTS0) and up to 22 kHz/cm^2 in the mTOF stop wall matching the design requirements of the CBM STS [1] as well as the CBM TOF [5] detector system. Here, δ-electrons enhance the hit rate within the first mSTS station by a factor of about 3.

The free-streaming DAQ system

The mCBM design focuses on the system performance aspect integrating existing (or currently under construction) prototype modules of all CBM detector subsystems into a common, high-performance free-streaming data acquisition (DAQ) system. The detector stations will be equipped with final readout electronics containing ultra-fast and radiation-tolerant ASICs as front-end chips followed by CERN GBTx-based radiation-tolerant data aggregation units. Further down-stream, the data streams are handled by Data Processing Boards (DPB) containing powerful FPGAs and are forwarded via FLES Input Boards (FLIB), a PCIe based FPGA board, to a large-scale computer farm, the First-Level Event Selector (mFLES, see [14]), which will perform on-line track and event reconstruction and selection, see Fig. 3.

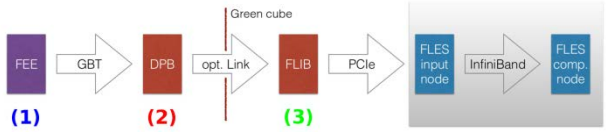

Figure 3: Envisaged mCBM readout chain for the startup phase, based on DPB and FLIB. The mCBM subsystems are equipped with individual front-end electronics FEE (1). These front-ends are interfaced by the GBTx ASIC, which forwards the detector data via optical GBT link. All GBT links are received by the DBP layer located at 50 m distance in the DAQ container (2). The DPB is a FPGA based board which allows for subsystem specific pre-processing of the arriving data stream. A long distance optical link connects the DPB output to the FLIB board installed in the FLES input node in the Green IT Cube (3).

The CBM detector front-ends are time-synchronized to the nanosecond level by the Timing and Fast Control (TFC) system. The detector front-end digitizes signals above threshold and assigns a time stamp to the hit. This data is then forwarded via an electrical connection to the GBTx readout board, where the electrical signals acquired through a large number of e-links are converted and merged into an optical GBT link operating at 4.48 Gbit/s. These GBT links are the detector interface to the Data AcQuisition (DAQ) chain.

On the road towards the full CBM DAQ system the mCBM DAQ system will be deployed in two phases. During phase I, the GBTx-based subsystems (mSTS, mMUCH, mTRD and mTOF) will be read out using already available readout chains based on existing prototype implementations of DPB and FLIB, see Fig. 3.

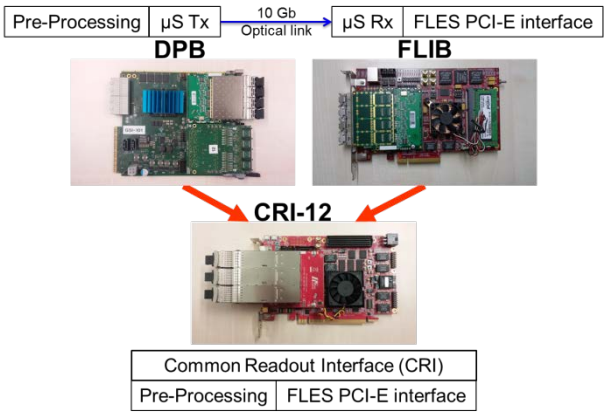

Figure 4: Upgrade of the mCBM DAQ in 2019.

As current prototype hardware, an AMC FMC Carrier Kintex (AFCK) board [15] is used for the DPB, a HiTech Global HTG-K700 PCIe board for the FLIB. Both boards are based on a Xilinx Kintex-7 FPGA. In phase II, DPB and FLIB will be replaced by a prototype of the Common Readout Interface (CRI) (see Fig. 4) in the FLES input stage, as it is foreseen for the CBM experiment. In addition, the mCBM subsystems (mRICH, mPSD) readout with FPGA TDCs chains will be added to the DAQ setup in 2019.

Reconstruction of the experimental area

The installation site for the mCBM test-setup is the detector test area named HTD in the GSI nomenclature (see Fig. 5) situated at the beam entrance of the experimental area cave-C (HTC) hosting the nuclear structure experiment R^3B. Although the space is very limited in the HTD area, the compact mCBM setup measuring a full length of about 4 m will fit into the HTD cave.

The arrangement of the HTD cave for the mCBM test-setup depends substantially on the incident angle of the beam as shown in Fig. 5. This also affects shielding measures which become necessary to make high-rate beam tests feasible up to CBM design collisions rates. Many iterations of radiation level simulations had been carried out using the FLUKA software package to fulfil the radiation safety requirements [16]. As one of the shielding measures, in particular to protect the R^3B experiment located in cave-C, a sandwich-like beam dump has been constructed consisting of 12x 12cm thick steel plates covered by 80 cm thick concrete blocks as visible in Fig. 6. A beam hole has been drilled up to the steel core (see Fig. 5) which will be blocked after irradiation.

Additional concrete blocks embedded into the chicane entrance have been placed directly in front of the R^3B target region (see Fig. 5 and 7). To block access into the HTD cave after high-rate beam-tests have taken place, a lockable entrance door is being installed. Up to four additional concrete layers with a thickness of 0.8 m each will be placed on top of the HTD cave ceiling.

As illustrated in Fig. 5, the incoming beam will be either transported to the R^3B experiment or deflected to the mCBM setup by a switching magnet (dipole magnet) mounted directly in front of cave-C carrying the name HTD MU1 in the GSI nomenclature. To date, beams had been deflected at an effective angle of 14.5° corresponding to an magnetic rigidity of Bρ = 10 Tm. Accordingly, the maximum kinetic energy for heavy projectiles like Au had been limited to 0.45 AGeV generating unrealistic conditions due to a large number of low-momentum fragments emitted during the collision. In order to exploit the full beam energy range of SIS18 we are going to exchange the vacuum chamber of the switching magnet by a spare chamber with vacuum outlets for 0° and 7.5°. With the given magnetic induction, beams will be bend on a radius of ρ = 11.25 m at top SIS18 energy which results to an effective deflection angle of 8.0°.

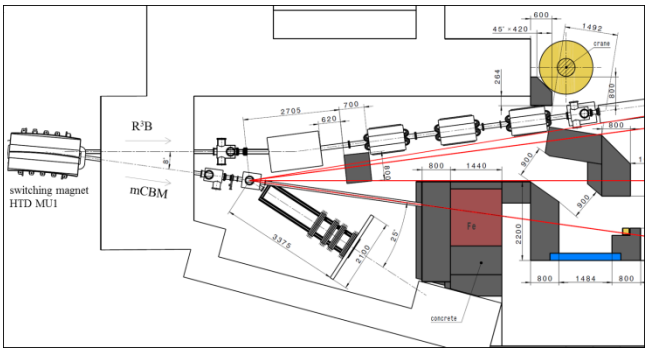

Figure 5: The modified mCBM cave (HTD) at the SIS18 facility of GSI/FAIR (as of August 31, 2017).

Figure 6: The Iron core of the beam dump is prepared for concrete pouring.

Figure 7: Chicane entrance to the mCBM cave (HTD).

 DOI:10.15120/GR-2018-1

Benchmarking the mCBM test-setup

To verify the performance of the CBM data taking concept the mCBM setup will be used to reconstruct physics observables that can be compared to published data. A feasibility study with the mCBM setup was performed using the Λ production probability in heavy-ion collisions as a benchmark observable. At SIS18 beam energies Λ baryons are produced close to or below the free NN production threshold. Thus their production probability is rather small posing a CBM-like challenge to the reconstruction and se- lection task.

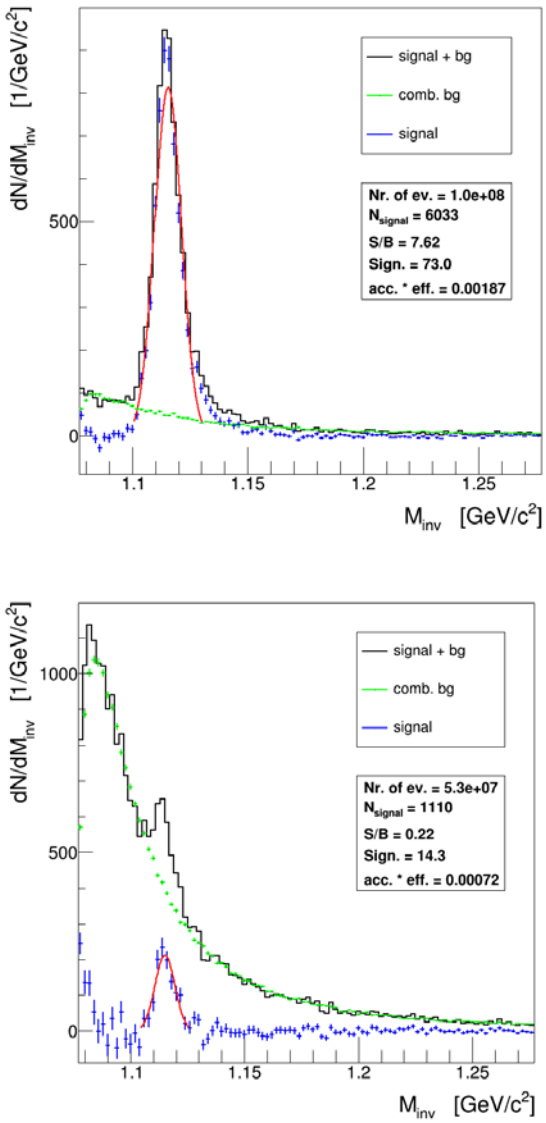

Figure 8: Λ-identification in minimum bias UrQMD events in Ni+Ni collisions at 1.93 AGeV (top) and in Au+Au at 1.24 AGeV (bottom). Invariant mass distributions are shown for (π-p) pair combinations (combinatorics) within events (black line, signal + bg), for pair combinations from mixed events (green symbols, comb. bg) and for the resulting distribution after subtraction (blue symbols, signal). Statistics information is obtained from a Gaussian fit to the subtracted distribution (red line).

Since mCBM does not include a magnetic field for momentum measurement, the reconstruction has to be done via time-of-flight (TOF) and track topology, assuming the pion and proton mass for (π-p) pair candidates. For simplicity, only STS and TOF hits are considered for the reconstruction algorithm. As geometry, the most recent mCBM setup has been used within the MC simulation as it is depicted in Fig. 1. Fig. 8 demonstrates that the limited information available is sufficient for Λ reconstruction. Improvements are certainly possible by tuning the selection cut values. As simulation input, 10^8 minimum bias events of the reactions Ni+Ni at an incident energy of 1.93 AGeV and $5.3 \cdot 10^7$ minimum bias events of Au+Au collisions at 1.24 AGeV have been generated with the UrQMD transport model [17]. The corresponding phase space coverage (efficiency in z-direction) for Ni+Ni collisions at 1.93 AGeV is shown in Fig. 9 demonstrating that the acceptance of mCBM is limited to a small angular range close to mid-rapidity.

For both benchmark collision systems published data from the FOPI collaboration are available in [18] as well as from the HADES collaboration in [19] that the mCBM results can be quantitatively compared to. It is worth noting that the technical goal and challenge is to reconstruct the invariant mass distributions shown in Fig. 8 within a time period of about 10 s data taking at SIS18, assuming 10^7 nucleus-nucleus collisions per second (10^8 ions per second bombarded on a 10 % interaction target).

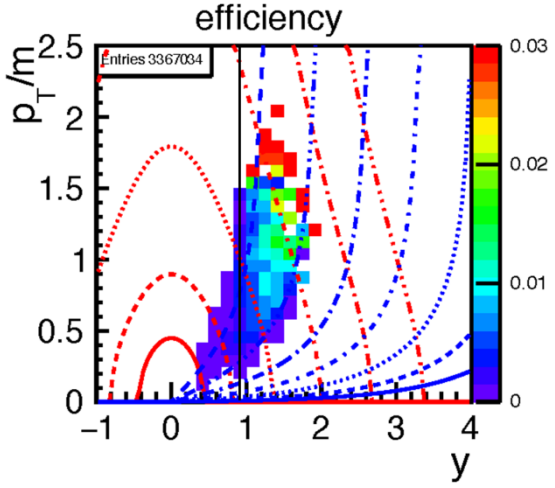

Figure 9: Efficiency of reconstructed Λ - baryons with mCBM produced in Ni+Ni collisions at 1.93 AGeV (input: events generated with UrQMD). Red and blue lines indicate constant laboratory momenta and laboratory polar angles, respectively. The black line marks mid-rapidity.

mCBM beamtime

Mid of 2017 a beamtime proposal had been submitted to the General Program Advisory Committee of GSI/FAIR (G-PAC) for the year 2018 (”development & commissioning”) with the focus on data transport, the data analysis as well as detector tests, and for the year 2019 (”approaching full performance”) implying the completion of subsystems, the high-rate data transport and data processing incl. online reconstruction. The applied beamtime has been fully granted by the G-PAC in September 2017.

All the background rejection strategies necessary to reconstruct rare probes with CBM at SIS100 can be prepared and exercised with mCBM. In addition, if the technical goals of mCBM are achieved, a measurement of the Λ production excitation function should become feasible. This was not yet measured in the SIS18 beam energy range thus offering a unique opportunity to contribute to world data, although the covered phase space is limited and therefore systematic errors become large when extrapolating to unmeasured regions.

The successful implementation and demonstration of the technical capabilities would also open the road to more relevant physics observables like the measurement of light hypernuclei. The beam time request for more physics oriented observables will be placed in the next beamtime period from 2020 – 2021, once the preliminary results are supporting the high expectations.

References

[1] J. Heuser, W. F.J. Müller, V. Pugatch, P. Senger, C.J. Schmidt, C. Sturm and U. Frankenfeld, Technical Design Report for the CBM Silicon Tracking System (STS),GSI-2013-05499, http://repository.gsi.de/record/54798

[2] S. Chattopadhyay, Y. P. Viyogi, P. Senger, W. F.J. Müller and C. J. Schmidt, Technical Design Report for the CBM: Muon Chambers (MuCh), GSI-2015-02580, https://repository.gsi.de/record/161297

[3] C. Höhne et al., Technical Design Report for the CBM Ring Imaging Cherenkov Detector (RICH), GSI-2014-00528, http://repository.gsi.de/record/65526

[4] C. Blume et al., Technical Design Report for the CBM Transition Radiation Detector (TRD), to be published

[5] N. Herrmann et al., Technical Design Report for the CBM Time-of-Flight System (TOF), GSI-2015-01999, https://repository.gsi.de/record/109024

[6] F. Guber and I. Selyuzhenkov, Technical Design Report for the CBM Projectile Spectator Detector (PSD), GSI-2015-02020 , https://repository.gsi.de/record/109059

[7] L. Radulescu, D. Emschermann, and A. Bercuci, CAD integration of the mCBM subsystems, CBM Progress Report 2017, 2018, DOI 10.15120/GSI-2018-00485

[8] O. Vasylyev et al., Progress with the integration of the mCBM Mini Silicon Tracking System, CBM Progress Report 2017, 2018, DOI 10.15120/GSI-2018-00485

[9] C. Ghosh et al., Development of a MUCH Cooling system for mCBM, CBM Progress Report 2017

[10] I. Deppner , N. Herrmann , and the CBM TOF working group, Time Of Flight Detector - Summary, CBM Progress Report 2017, 2018, DOI 10.15120/GSI-2018-00485

[11] The CBM eTOF working group, The TOF FAIR Phase 0 project - eTOF at STAR, CBM Progress Report 2017, 2018, DOI 10.15120/GSI-2018-00485

[12] G. Pitsch , S. Lebedev, and C. Höhne, Monte-Carlo Simulations of a mRICH detector with aerogel radiator in mCBM, CBM Progress Report 2017, 2018, DOI 10.15120/GSI-2018-00485

[13] F. Guber, mPSD at mCBM, CBM Progress Report 2017, 2018, DOI 10.15120/GSI-2018-00485

[14] D. Hutter , J. de Cuveland , and V. Lindenstruth, Preparations for the mCBM FLES Setup, CBM Progress Report 2017

[15] W.M. Zabołotny and G. Kasprowicz, "Data processing boards design for CBM experiment", Proc. SPIE 9290 (2014) 929023, doi:10.1117/12.2073377

[16] A. Senger et al. (CBM Collaboration), Concrete shielding and beam dump for mCBM, CBM Progress Report 2017, 2018, DOI 10.15120/GSI-2018-00485

[17] M. Bleicher et al., Relativistic Hadron-Hadron Collisions in the Ultra-Relativistic Quantum Molecular Dynamics Model, J. Phys. G: Nucl. Part. Phys. 25 (1999) 1859-1896

[18] M. Merschmeyer et al. (FOPI collaboration), K0 and Λ production in Ni+Ni collisions near threshold, Phys. Rev. C 76 (2007) 024906

[19] H. Schuldes et al. (HADES collaboration), Studying Strangeness Production with HADES, Web of Conferences 171, 01001 (2018), SQM2017

Experiment beamline: mCBM@SIS18
Experiment collaboration: CBM
Experiment proposal: S471
Accelerator infrastructure: SIS18 / HEST
PSP codes: 1.1.1
Grants:
GSI Helmholtzzentrum für Schwerionenforschung GmbH
Facility for Antiproton and Ion Research,
Helmholtz Gemeinschaft,
BMBF No. 05P12VHFC7, 05P2015, 05P15PXFCA, 05P15RGFCA, 05P12RGFCG, 05P15RFFC1, 05P12VTFCE, 05P15VHFC1, 05P15PMFC1, 05P16VTFC1, 05P16PMF1, 05P16PMFC1, 05P15ZAFC1,
HIC for FAIR Helmholtz International Center,
HGS-HIRe for FAIR,
Hessian Initiative for Excellence (LOEWE),
Cremlin - Connecting Russian and European Measures for Large-scale Reasearches Infrastructure,
European Union's Horizon 2020 research and innovation programme under grant agreement No.654166 and 654168, Helmholtz-YIG grant No.VH-NG-823,
Humboldt foundation, Germany
Strategic university co-operation with:
Darmstadt, Frankfurt-M, Gießen, Heidelberg

* This report is also part of the CBM Progress Report 2017, 2018, DOI 10.15120/GSI-2018-00485

D mesons Langevin propagation at SIS300-FAIR

G. Inghirami [1,2,3,4], H. Van Hees[1,2], S. Endres[1,2], J. Torres-Rincon[5] and M. Bleicher[1,2,3,4]

[1]FIAS, Frankfurt am Main, DE; [2]Goethe-Universität, Frankfurt am Main, DE; [3]GSI, Darmstadt, DE;
[4]J. von Neumann Institute for Computing, Jülich, DE; [5]Stony Brook University, Stony Brook, New York, USA

Heavy quarks represent an excellent tool to probe the properties of the medium which is supposed to form in relativistic heavy ion collisions, because they are produced in the very initial stages after the collision and their number is conserved until the hadrons they form decay by weak interaction, long time after the kinetic freezeout. Since their masses are considerably larger than the light quark masses, we can model their propagation into the medium by adopting a Langevin approach. In this work we perform the Langevin propagation of c and anti-c quarks in fixed target Au-Au collisions, with 25 AGeV beam energy, in the range of the future FAIR facility. In our simulations we neglect the back reaction of charm quarks and D mesons on the medium, allowing for the simultaneous propagation of many charm quarks at the same time, whose initial momentum distribution is computed by using Pythia 8.2. We compute the evolution of the background medium using both the UrQMD/hybrid [1] and the UrQMD/coarse graining [2] approaches, running simulations at fixed impact parameters b = 3 fm and b = 7 fm. We perform the hadronization by adopting an instantaneous coalescence model [3] in momentum space combined with Peterson fragmentation. We consider only the formation of D^+, D^0 mesons and their antiparticles. We take into account the effects of the finite baryon chemical potential on the values of the transport coefficients through a fugacity factor. The drag and diffusion coefficients in the partonic phase are computed within a resonance model [4], while the description of how the coefficients are derived in the case of D mesons can be found in ref. [5]. We study how variations in the centrality class and in the conditions for charm quark hadronization influence the elliptic flow and the nuclear modification factor of the final D and anti-D mesons.

We find that most of the final elliptic flow of D and anti-D mesons is built during the partonic phase, while the subsequent hadronic interactions seem to have a limited influence. Moreover, we find that the model of the dynamics of the medium and the hadronization procedure have a large impact on the magnitude and on the transverse momentum dependence of the elliptic flow and of the nuclear modification factor.

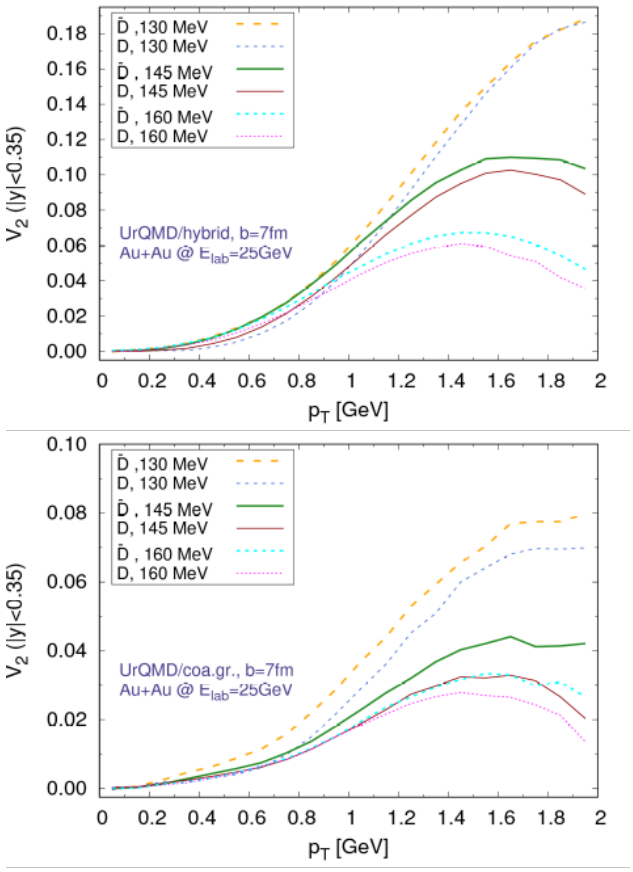

Figure 1: Elliptic flow of D and anti-D mesons (|y| < 0.35) within the UrQMD/hybrid (top) and UrQMD/coarse graining (bottom) approaches. Here we show the dependence on the hadronization temperature in Au+Au collisions at Elab = 25 AGeV at a fixed impact parameter b = 7 fm.

References

[1] H. Petersen, J. Steinheimer, G. Burau, M. Bleicher and H. Stöcker, Phys. Rev. C 78, 044901 (2008)

[2] S. Endres, H. van Hees, J. Weil and M. Bleicher, Phys. Rev. C 92, 014911 (2015)

[3] V. Greco, C. M. Ko and R. Rapp, Phys. Lett. B 595, 202 (2004)

[4] H. van Hees and R. Rapp, Phys. Rev. C 71, 034907 (2005)

[5] L. Tolos and J. M. Torres-Rincon Phys. Rev. D 88, 074019 (2013)

Grants: COST Action CA15213 (THOR)

Strategic university co-operation with: Frankfurt-M

CBM computing – progress, status and outlook

J. de Cuveland[1], V. Friese[2], P.-A. Loizeau[2], F. Uhlig[2], M. Zyzak[2]
for the CBM Computing Working Group

[1]FIAS, Frankfurt, Germany; [2]GSI, Darmstadt, Germany

The development of CBM software has, over the years, concentrated on simulation of nuclear collision events in the CBM detector setup, and reconstruction and analysis of the simulated data. The corresponding tools were widely used for studying the physics performance of the CBM detector.

With the advent of mCBM, which will start taking data in August 2018, new challenges appeared, which have to be met on a rather short timescale. mCBM will allow to test the entire data chain, from the front-end electronics through the DAQ chain to online and offline processing of experiment data on CPU. This will allow to scrutinise existing software concepts, but also enforces to accelerate the process of moving simulation and reconstruction from the event-by-event case to the handling of free-streaming data, corresponding to the real situation for CBM and mCBM. Moreover, issues not addressed so far, like the software needed to set-up, run and control the experiment, and, most of all, a framework concept of processing data in real-time, suddenly become very urgent.

To meet these challenges organisationally, the CBM software activities were structured and defined in a project-like manner, with the aim to distribute responsibilities, assess manpower, planning, timelines and milestones, and identify critical items and shortage of workforce. The following Computing Projects were defined (see Fig. 1):

- Experiment and Detector Control Systems (EDC): tools to configure and monitor detectors and DAQ
- Online Data Management (ODM): software to operate the online computing farm, receive data from the experiment, build time slices and deliver them to the compute nodes
- Data Processing Framework (DPF): the environment for data processing both online and offline
- Data Analysis Algorithms (ALG): algorithms for event reconstruction and common data analysis
- Simulation Software (SIM): enable detector simulation on the same level as real experiment raw data
- Offline Analysis Environment (OAE): develop strategies and tools for the offline analysis of large-scale data
- Software Development Infrastructure (INF): provide and maintain tools for collaborative software development and maintenance

The platform for coordination of and communication between the projects is the newly established Computing Board. In the following, we briefly report on the status and progress following the project structure.

Experiment and Detector Control system

The detector control was until now driven by beam-time activities and therefore mostly concerned systems with single detector type [1-3]. Following the establishment of the Computing Board, work is ongoing to define the tasks, interfaces and general specifications of the slow-control, detector-control and central experiment control systems. Prototypes of these systems will help for the operation of mCBM phase I and are necessary for efficient data taking with mCBM phase II.

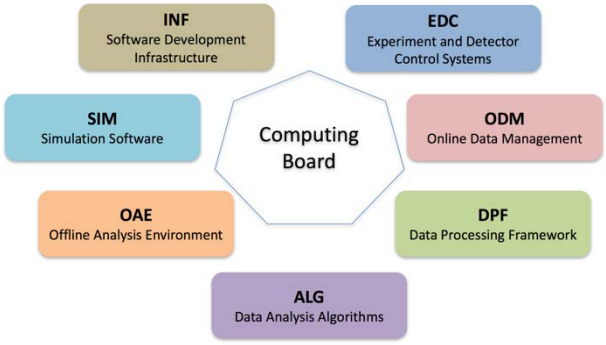

Figure 1: Computing project structure

Online Data Management

A demonstrator software that implements time slice building as well as the interfaces to detector links and online processing has been available for several years. This software, named *FlesNet* has already been used for online data taking in various CBM detector test setups and beam tests. It is still evolving, with recent work focusing on operational improvements for small and medium-sized setups. This includes the addition of a ZeroMQ-based transport complementing the existing RDMA-based transports [4].

With regard to the full SIS-100 setup, the scalability of the time slice building has been improved, including the demonstrator implementation of a new data-flow scheduler [5]. The work of the near future will cover additional features and tools that will also be beneficial to the upcoming operation of mCBM.

Data Processing Framework

The ROOT-based software framework employed by CBM for many years now allows to simulate, reconstruct and analyse physics events in an integrated environment. It, however, provides no inherent mechanism to parallelise the execution of tasks and thus make full use of the available computing architectures. This strongly limits its applicability for real-time data processing on the CBM compute nodes. First studies to introduce parallelism schemes into *CbmRoot* were undertaken [6, 7], but showed little performance gain owing to the structure of the reconstruction processing graph. In the future, the possibility to use the message-queue based *FairMQ* scheme, developed by the Scientific Computing group of GSI as extension to *FairRoot*, will be investigated.

 DOI:10.15120/GR-2018-1

Databases for various purposes (configuration, conditions, components) will be important ingredients to the framework. *FairDB* is currently used for managing the hardware component properties in several detector systems and may also be usable for other purposes [8].

Data Analysis Algorithms

The core reconstruction algorithm, the track finding in the STS, was already enabled to operate on free-streaming data. The event-building procedure from reconstructed STS tracks is also available and was tested with physics analysis [9]. The proper time-based input from cluster and hit finding, however, is currently only available for the STS and MUCH systems [7, 10]. Thus, current efforts are devoted to extend the existing time-based reconstruction to the downstream detectors (global tracking). Progress was made for tracking in the muon system [11, 16] and in the TRD [12]. In addition, the particle identification potential for light nuclei, relevant for the study of e.g., hyper-nuclei production, was investigated using the energy loss in the STS [13] and in the TRD [14]. Moreover, a first version of track finding in mCBM, which differs from the full CBM in the track model, was made available [15].

Development of the time-based procedure for reconstruction of global tracks is in progress. Two approaches are being considered at the moment: based on the *littrack* and the CA track finder algorithms. The *littrack* method is the current standard, and addition of the time measurement to the reconstruction scheme is a straightforward solution. However, it is based on the track following algorithm using STS tracks as seeds, which makes it complicated to be applied for the detector alignment task. In its turn, the CA track finder in STS is already fully adapted for time-based reconstruction and expansion of the method to the downstream detectors is currently being implemented [16]. The task of the time-based global track finder requires realistic description of the time response of cluster and hit finding algorithms, which will be addressed in the nearest future. Based on this realistic input, the existing solutions for global tracking will be compared w.r.t. performance in order to arrive at an optimal solution.

Simulation Software

The two major ingredients for simulations are the description of the detector geometry and a model for the detailed detector response (digitizer). The detector geometries for CBM were consolidated; by now, all detector systems deliver the geometry in the ROOT *TGeoManager* format as agreed on for standalone visualisation and management through a database (see [17-19]). Geometry descriptions for all detector system participating in mCBM are also available. In order to manage the increasing number of geometry versions for the detector system for different contexts / setups and provide them in a controlled and user-friendly way, the development of a Geometry Database was continued; a prototype is now available for testing [20].

Time-based version of all digitizers were provided (see [18, 21]), which is of particular importance for the modelling of the actual data stream from both mCBM and CBM. Together with a (simplified) software representation of the time-slice building, the simulation output is now logically equivalent to the raw data expected from the data acquisition. It is, however yet on the *digi* (ROOT) level and does not include all details of the time slice building (e.g., micro-slice sub-structure). Similarly, not all relevant features (e.g., data loss due to pile-up from different events) are yet included in all digitizers; this will be the task for the immediate future.

The next issues to be addressed by simulation software are thus: the proper treatment of inter-event pile-up in the digitizers, the inclusion of not event-correlated background sources into the simulations (see [22, 23]) and the description of the data stream in the actual raw data format.

Offline Analysis Environment

Considerations to organise the offline analysis of the huge amount of data CBM will archive when starting operations in 2024 have not started yet in earnest. A strategy will be developed in close cooperation with the other FAIR experiments, in particular with PANDA as the other data-intensive experiment, and with FAIR/GSI-IT. First steps to develop a common FAIR computing model, of which the CBM computing model will be one part, will be taken in 2018, with the aim to arrive at a Technical Design Report in 2020.

Software Development Infrastructure

The basic tools to enable an effective and collaborative software development are in place and operational since several years.

- Software distribution: *CbmRoot*, comprising simulation, reconstruction and analysis software, is distributed through a *subversion* repository hosted on a GSI server. Several packages (*KFParticle*, *KFParticleFinder*, *FlesNet*), are hosted separately on *git* servers and are integrated into *CbmRoot* in the build process. The movement of the entire CBM software to a *git* repository is one of the tasks for the next future.
- Build system: We use *CMake* to build *CbmRoot*, which takes also care of the integration of external packages. Shell scripts for the installation of external packages and of *FairRoot* are provided. The installation is supported on all Linux flavours as well as for OS X.
- Documentation: By convention, documentation is provided in-code in *Doxygen* format. The documentation is generated nightly on a GSI server, which provides a browser-based output [24]. Additional requirements on documentation are to be defined by the Computing Projects.
- Software integrity management: the possibility to perform regular tests (nightly or on commit) is provided through a *CDash* system. Tests are to be defined by the Computing Projects. The test results are furnished on a web server [25].
- Project management and communication: The collaborative platform for software development in

CBM is a *Redmine* instance [26]. It integrates a browser front-end to the repository, systems for issues, news, forum and Wiki, and project planning facilities. The *Redmine* system is also used for some hardware projects.

The development tools and the deployment of servers are subject to constant maintenance and further development following the needs of the Computing Projects.

This report is also part of the CBM Progress Report 2017 (doi:10.15120/GSI-2018-00485).

References

[1] P. Klaus et al., *The Detector Control System for the MVD prototype PRESTO*, CBM-PR2017*, p. 12

[2] J. Bendarouach and C. Höhne, *Design of a control and monitoring system for the mirror alignment of the CBM RICH detector*, CBM-PR2017, p. 59

[3] V. Negi, J. Saini and S. Chattopadhyay, *Design and development of error resilient control system of Low Voltage Distribution Board for CBM-MUCH detector*, CBM-PR2017, p. 79

[4] J. de Cuveland et al., *A FLESnet transport using ZeroMQ*, CBM-PR2017, p. 129

[5] F. Salem et al., *Data-flow scheduling for a scalable FLESnet*, CBM-PR2017, p. 130

[6] M. Prokudin, *Parallelization of CbmRoot at task level*, CBM-PR2017, p. 132

[7] V. Singhal et al., *Parallelization of cluster and hit finding for the CBM-MUCH*, CBM-PR2017, p. 144

[8] D. Bertini and E. Lavrik, *Progress with FairDB development*, CBM-PR2017, p. 133

[9] V. Akishina et al., *Reconstruction of time-slices in CBM at high interaction rates*, CBM-PR 2017, p. 145

[10] V. Friese, *Time-based cluster finding in the CBM-STS detector*, CBM-PR2017, p. 143

[11] A. Zinchenko and V. Ladygin, *Application of the vector finding-based track reconstruction method for the CBM muon setup*, CBM-PR2017, p. 146

[12] O. Derenoskaya, T. Ablyazimov and V. Ivanov, *Towards $J/\psi \to e^+e^-$ triggering with the CBM-TRD*, CBM-PR2017, p. 148

[13] H. Malygina et al., *Investigation into the particle identification potential of the CBM-STS*, CBM-PR2017, p. 160

[14] S. Gläßel et al., *Hadron identification via energy loss measurements with the TRD*, CBM-PR2017, p. 156

[15] T. Ablyazimov, V. Friese and V. Ivanov, *Using the binned tracker in mCBM*, CBM-PR2017, p. 189

[16] V. Akishina, I. Kisel and M. Zyzak, *Kalman Filter track fit for the CBM STS and MUCH detector systems*, CBM-PR2017, p. 147

[17] P. Klaus et al., *Update on the CBM MVD geometry*, CBM-PR2017, p. 135

[18] L. Lebedev, E. Ovcharenko and C. Höhne, *RICH software status*, CBM-PR2017, p. 138

[19] O. Singh et al., *Description of the CBM-MUCH geometry in ROOT format*, CBM-PR2017, p. 140

[20] E. Akishina et al., *Geometry database for the CBM experiment*, CBM-PR2017, p. 142

[21] A. Bercuci et al., *Time-based CbmRoot simulations of the Bucharest TRD prototype for mCBM*, CBM-PR2017, p. 186

[22] V. Friese, *Implementation of electronic noise in the simulation of the CBM-STS*, CBM-PR2017, p. 137

[23] A. Senger, *Time-based track reconstruction in STS with δ-electrons*, CBM-PR2017, p. 136

[24] http://cbmroot.gsi.de/cbm-doc/daily/html/index.html

[25] https://cdash.gsi.de/index.php?project=CbmRoot

[26] https://redmine.cbm.gsi.de/projects/cbmroot

.

* I. Selyuzhenkov and A. Toia (eds.), CBM Progress Report 2017, Darmstadt 2018, ISBN 978-3-9815227-5-4, doi:10.15120/GSI-2018-00485